ITPK1 is an $InsP_6$/ADP phosphotransferase that controls systemic phosphate homeostasis in Arabidopsis

Esther Riemer[1], Debabrata Laha[2,#], Robert K. Harmel[3,#], Philipp Gaugler[1,#], Verena Pries[1], Michael Frei[1], Mohammad-Reza Hajirezaei[4], Nargis P. Laha[1], Lukas Krusenbaum[1], Robin Schneider[1], Henning J. Jessen[5], Adolfo Saiardi[2], Dorothea Fiedler[3], Gabriel Schaaf[1]*, Ricardo F.H. Giehl[4]*

ORCID IDs:

DL: 0000-0002-7823-5489, RKH: 0000-0003-4413-7730, NPL: 0000-0002-7744-1408, HJJ: 0000-0002-1025-9484, AS: 0000-0002-4351-0081, DF: 0000-0002-0798-946X, GS: 0000-0001-9022-4515, RFHG: 0000-0003-1006-3163

[1] Department of Plant Nutrition, Institute of Crop Science and Resource Conservation, Rheinische Friedrich-Wilhelms-Universität Bonn, 53115 Bonn, Germany.

[2] Medical Research Council Laboratory for Molecular Cell Biology (MRC-LMCB), University College London, London WC1E 6BT, United Kingdom.

[3] Leibniz-Forschungsinstitut für Molekulare Pharmakologie, 13125 Berlin, Germany and Department of Chemistry, Humboldt Universität zu Berlin, 12489 Berlin, Germany.

[4] Department of Physiology & Cell Biology, Leibniz-Institute of Plant Genetics and Crop Plant Research, 06466 Gatersleben, Germany.

[5] Department of Chemistry and Pharmacy and CIBSS-Centre for Integrative Biological Signalling Studies, Albert-Ludwigs University Freiburg, 79104 Freiburg, Germany.

[#] These authors contributed equally to this work.

*To whom correspondence and material requests should be addressed: gabriel.schaaf@uni-bonn.de and giehl@ipk-gatersleben.de.

ABSTRACT

In plants, phosphate (P_i) homeostasis is regulated by the interaction of P_i starvation response transcription factors (PHRs) with stand-alone SPX proteins, which act as sensors for inositol pyrophosphates (PP-InsPs). Recently, ITPK1 was shown to generate the PP-InsP $InsP_7$ from $InsP_6$ *in vitro*, but the importance of this activity in P_i signaling remained unknown. Here, we show that uncontrolled P_i accumulation in ITPK1-deficient plants is accompanied by impaired P_i-dependent $InsP_7$ and $InsP_8$ synthesis. Reciprocal grafting demonstrates that P_i starvation responses are mainly controlled by ITPK1 activity in shoots. Nuclear magnetic resonance assays and PAGE analyses with recombinant protein reveal that besides $InsP_6$ phosphorylation, ITPK1 is also able to catalyze ATP synthesis using 5-$InsP_7$ but not any other $InsP_7$ isomer as a P-donor when ATP is low. Additionally, we show that the dynamic changes in $InsP_7$ and $InsP_8$ to cellular P_i are conserved from land plant species to human cells, suggesting that P_i-dependent PP-InsP synthesis is a common component of P_i signaling across kingdoms. Together, our study demonstrates how P_i-dependent changes in nutritional and energetic states modulate ITPK1 activities to fine-tune the synthesis of PP-InsPs.

INTRODUCTION

In order to maintain cellular P_i homeostasis, plants have evolved complex sensing and signaling mechanisms that adjust whole-plant P_i demand with external P_i availability. Although many molecular players involved in these responses have been identified, the exact mechanism of P_i sensing in complex organisms, such as plants, still remains largely unknown. In the model species *Arabidopsis thaliana*, the MYB transcription factors PHOSPHATE STARVATION RESPONSE 1 (PHR1) and its closest paralog PHR1-LIKE1 (PHL1) control the expression of the majority of P_i starvation-induced (PSI) genes and influence numerous metabolic and developmental adaptations induced by P_i deficiency[1, 2]. In agreement with their regulatory function, a subset of P_i deficiency-induced genes is deregulated in *phr1 phl1* mutants. However, since *PHR1* itself is not transcriptionally regulated by P_i deficiency, the existence of a post-translational control of PHR1 has been proposed[1]. Emerging evidence indicates that a class of stand-alone SPX proteins negatively regulate the activity of PHR transcription factors in different plant species[3, 4, 5, 6, 7, 8]. According to these studies, when plants have access to sufficient P_i, SPX proteins bind with high affinity to PHRs, thereby preventing binding of these transcription factors to DNA. Under low P_i, the affinity of SPX proteins towards PHRs is decreased, thus allowing these transcription factors to activate their transcriptional targets[4].

The *in vivo* interaction of PHR1 and SPX1 is influenced by P_i[3, 4, 5], suggesting that this mechanism could represent a direct link between P_i perception and downstream signaling events. However, the dissociation constants for P_i itself in a SPX-PHR complex ranged from 10 mM to 20 mM[3, 4, 5], while P_i levels of only 60 µM to 80 µM have been recorded in the cytosol of plant cells[9]. A later study, demonstrated that SPX domains can actually act as receptors for inositol pyrophosphates (PP-InsPs) and isothermal titration calorimetry experiments revealed that 5PP-InsP_5 (hereafter referred to as 5-InsP_7) interacted more strongly

with SPX domains than P_i[10]. In these assays, interaction of rice OsPHR2 and OsSPX4 was promoted at 5-$InsP_7$ concentrations as low as 20 µM[10]. Although the isomeric nature of plant $InsP_7$ in vegetative tissues remains unknown, it has been proposed that the activity of PHRs is regulated by direct interaction with PP-InsPs. In support of this hypothesis, an Arabidopsis mutant for *INOSITOL PENTAKISPHOSPHATE 2-KINASE* (*IPK1*), which is compromised in the synthesis of the PP-InsP precursor inositol hexakisphosphate ($InsP_6$), exhibits constitutive PSR and increased P_i accumulation when grown on sufficient P_i availability[11, 12]. More recently, other mutants with compromised synthesis of PP-InsPs have been shown to exhibit disturbed PSR and P_i over-accumulation phenotypes[13, 14, 15], and it was observed that the levels of different inositol polyphosphates (InsPs) are significantly altered in P_i-deficient plants[13, 14]. Interestingly, polyacrylamide gel electrophoresis (PAGE) analyses revealed that $InsP_8$ levels increase in P_i-sufficient plants and decrease as plants are exposed to P_i deficiency[14], suggesting that the enzymes involved in the synthesis of PP-InsPs could act as regulators of P_i homeostasis in plants. This regulation was first discovered in the yeast *Saccharomyces cerevisiae* in which cellular levels of PP-InsPs decrease when exposed to P_i-deficient medium[10, 16]. However, the biosynthetic pathway resulting in P_i-dependent PP-InsP synthesis still remains largely unresolved and it also remains unclear if this response is conserved in the plant lineage and across kingdoms.

In plants, synthesis of $InsP_8$ is mediated by VIH1 and VIH2[17], a class of bifunctional kinase/phosphatase enzymes[15] sharing homology to the yeast and animal Vip1/PPIP5Ks[17, 18, 19]. Although *vih1* and *vih2* single mutants do not exhibit impaired P_i accumulation[13], deletion of both VIHs results in severe growth defects and P_i overaccumulation[14, 15]. Since plant genomes do not encode homologues of the metazoan and yeast $InsP_6$ kinases IP6K/Kcs1, it has since long remained elusive how plants synthesize $InsP_7$. Using a yeast complementation assay, we recently identified Arabidopsis ITPK1 and ITPK2 as novel plant $InsP_6$ kinases and

99 demonstrated that ITPK1 generates the symmetric $InsP_7$ isomer 5-$InsP_7$, the major form
100 identified in seed extracts[20]. More recently, we further showed that $InsP_7$ and $InsP_8$ levels are
101 compromised in TPK1-deficient plants, demonstrating that ITPK1 functions as an $InsP_6$
102 kinase *in planta* [21]. Considering that $InsP_7$ is the precursor for $InsP_8$ synthesis, the next
103 challenge is to determine how $InsP_7$ levels respond to the plant's P_i status. A recent study
104 reported that $InsP_7$ levels increase in shoots of P_i-deficient Arabidopsis plants as determined
105 by HPLC analysis of [^{32}P]-P_i-labeled plant extracts[13]. However, this response is opposite to
106 what has been described in yeast[16] and mammalian cells[22] and is inconsistent with increased
107 $InsP_8$ levels detected by PAGE in P_i-sufficient Arabidopsis plants[14]. Considering that ^{32}P-
108 labeling entails complicated molecule assignment and does not provide a mass assay of the
109 inositol backbone but a readout for pyrophosphate moiety turnover, these results await
110 confirmation via alternative approaches. Importantly, it remains unclear whether ITPK1 and
111 ITPK2 contribute to PP-InsP synthesis in a P_i- and/or cellular energy status-dependent manner
112 and how the proposed regulatory activity of $InsP_8$ to suppress PSR might be deactivated once
113 plants experience P_i deficiency.

114 Here, we combine strong anion exchange chromatography (SAX)-HPLC analyses of [^{3}H]-
115 inositol-labeled seedlings and PAGE to investigate P_i-dependent changes in the levels of
116 $InsP_6$, $InsP_7$ and $InsP_8$ across diverse species and several *Arabidopsis* mutants. We
117 demonstrate that specifically in shoots, PP-InsPs decrease during P_i starvation and strongly
118 increase after P_i resupply. P_i-dependent regulation of PP-InsPs was also highly conserved
119 from diverse plant species to human cells. We find that ITPK1 is critical for the synthesis of
120 PP-InsPs involved in the regulation of P_i homeostasis. In addition, we demonstrate that
121 ITPK1-mediated conversion of $InsP_6$ to 5-$InsP_7$ requires high ATP concentrations and that
122 ITPK1 has ADP phosphotransferase activity under conditions of decreased adenylate energy
123 charge. These results provide a further link between P_i-dependent changes in nutritional and

124 energetic states with the synthesis of regulatory PP-InsPs. Finally, our study demonstrates that
125 ITPK1 activity in shoots regulates PSR responses in a PHR1/PHL1-dependent manner,
126 revealing that ITPK1 is a critical component of the systemic P_i sensing and signaling
127 mechanism in plants.

128

129 # RESULTS

130 ## Loss of ITPK1 but not ITPK2 affects P_i homeostasis in Arabidopsis

131 Previously, it has been reported that shoot P_i concentrations are significantly changed in a
132 number of InsP biosynthesis mutants grown in hydroponics[13]. We assessed the growth of
133 several of these mutants on soil and compared total P_i levels in shoots (measured with ICP-
134 OES) with that of WT and the P_i-overaccumulator *pho2-1*. We confirmed that *ipk1-1* and
135 *itpk1* plants accumulated significantly more total P_i in shoots, reaching levels comparable to
136 those detected in *pho2-1* (Fig. 1a and 1b). To a much lesser degree, shoot P_i levels were also
137 significantly increased in shoots of *mips1* and *vih2-4* plants, whereas P_i concentrations in all
138 other mutants assessed, including *itpk2-2*, were similar to their respective WTs. A full
139 elemental analysis indicated that the concentrations of other nutrients were largely unaffected
140 in shoots of *itpk1* plants as compared to WT (Suppl. Fig. 1). Total P_i levels were also
141 significantly increased in flowers and seeds of *itpk1* plants, although the relative changes were
142 less marked as those detected in rosette leaves (Suppl. Fig. 2). Excessive P_i accumulation
143 could be almost completely complemented in transgenic lines expressing the genomic *ITPK1*
144 fragment in the *itpk1* background (Fig. 1c and 1d), showing that P_i overaccumulation
145 phenotype was indeed associated with the loss of ITPK1.

146 To investigate whether P_i accumulation is dependent on external P_i availability, we cultivated
147 plants on agar plates supplemented with sufficient or insufficient P_i. A root phenotypical

148 analysis revealed that under sufficient P_i supply *itpk1* plants had shorter roots than WT plants,
149 a phenotype that was also largely rescued in the recomplemented lines (Fig. 1e and 1f)[21]. The
150 short-root phenotype of *itpk1* plants was also observed when plants were exposed to low P_i
151 supply in agar plates (Fig. 1e and 1f) or cultivated in hydroponics (Suppl. Fig. 3), and was
152 likely not associated with P_i overaccumulation, as the length of primary roots of *pho2-1* plants
153 was similar to WT (Suppl. Fig. 3). Furthermore, we found that increased total P_i accumulation
154 of *itpk1* plants was not detected in roots, while in shoots it was dependent on P_i availability
155 (Fig. 1g and 1h). The shoot P_i overaccumulation phenotype of *itpk1* has been associated with
156 defective down-regulation of PSRs in roots[13]. Our qPCR analysis confirmed that the
157 expression of many PSI genes was up-regulated in *itpk1* roots but only when plants were
158 grown under sufficient P_i or when P_i-deficient plants were resupplied with P_i for 6 hours
159 (Suppl. Fig. 4). Together, these results demonstrate that loss of ITPK1 but not ITPK2 affects
160 the regulation of PSR in plants.

161

162 **ITPK1 is required for P_i-dependent synthesis of PP-InsPs**

163 Recently, two studies have raised strong evidence for the role of $InsP_8$ in controlling P_i
164 homeostasis in plants[14, 15]. To further investigate which InsPs respond to rapid changes in the
165 plant's P_i status, we first performed SAX-HPLC analyses of extracts from [^{3}H]-inositol-
166 labeled WT seedlings. Of all InsPs detected, only one $InsP_3$ isomer, $InsP_6$ and the PP-InsPs
167 $InsP_7$ and $InsP_8$ decreased in response to P_i starvation and increased again when P_i was
168 resupplied to P_i-starved seedlings for 6 hours (Fig. 2a and 2b). Notably for $InsP_8$, P_i resupply
169 increased levels beyond those detected in seedlings continuously grown with sufficient P_i
170 (Fig. 2b).

In order to increase the throughput of $InsP_6$, $InsP_7$ and $InsP_8$ analysis and to allow assessing fully developed plants under more physiological conditions, we grew plants in hydroponics with aerated solution. Highly anionic InsPs and PP-InsPs extracted from plant tissues were purified by titanium dioxide (TiO_2)-based pulldown followed by separation via PAGE and subsequent visualization by Toluidine Blue and 4′,6-diamidino-2-phenylindole (DAPI) based on previously established protocols[23, 24, 25]. In agreement with our HPLC analyses, $InsP_6$, $InsP_7$ and $InsP_8$ signals in shoots of WT plants were strongly decreased when plants were deprived of P_i for 4 days (Fig. 2c and 2d). However, only $InsP_7$ and especially $InsP_8$ level were quickly restored by refeeding plants with P_i for 12 hours. Compared to WT, $InsP_7$ and $InsP_8$ levels were significantly lower in shoots of *itpk1* plants especially after P_i resupply (Fig. 2c and 2d). These results confirmed that ITPK1 functions as a cellular $InsP_6$ kinase *in planta* and suggested that an ITPK1-dependent $InsP_7$ pool is required and rate limiting for the efficient synthesis of $InsP_8$ under conditions of high P_i availability. In contrast to *itpk1*, PP-InsP levels were not compromised in the *itpk2-2* mutant (Suppl. Fig. 5a), further suggesting that ITPK1 can compensate for the loss of *ITPK2*. Notably, in roots of both WT and *itpk1* plants, $InsP_7$ and $InsP_8$ were barely detected by PAGE (Fig. 2e).

To further address the role of different InsPs in PSR, we analyzed the *itpk4-1* mutant, which was recently reported to display reduced levels of $InsP_5$[1/3-OH], $InsP_6$ and $InsP_7$ [13]. Whereas HPLC analysis of [^{3}H]-inositol-labeled seedlings confirmed the reported defects in $InsP_5$ [1/-OH] synthesis[21], our PAGE analyses did not detect any changes in $InsP_6$, $InsP_7$ nor $InsP_8$ levels in this mutant as compared to WT irrespective of the imposed P_i regime (Suppl. Fig. 5b and 5c). Thus, the undisturbed synthesis of PP-InsPs in *itpk4-1* plants may explain why this mutant shows no PSR phenotypes (Fig. 1b)[13].

Considering that only $InsP_7$ and $InsP_8$ responded to P_i, we then investigated the accumulation of these PP-InsPs in the P_i overaccumulator mutant *pho2-1*. We found that, compared to WT,

196 *pho2-1* plants accumulated much higher levels of $InsP_7$ and $InsP_8$, even when grown on low P_i
197 for 4 days (Fig. 2f). Notably, elemental analysis revealed that P_i levels in shoots of *pho2-1*
198 plants exposed to low P_i were still significantly higher than those detected in WT plants
199 grown under sufficient P_i (Fig. 2g). Together, these results indicate that the synthesis of PP-
200 InsPs is dependent on the internal, cellular P_i levels rather than external P_i availability.

201

202 **Synthesis of $InsP_7$ and $InsP_8$ relies on ITPK1 and VIH2 and on $InsP_6$**
203 **compartmentalization**

204 As suggested in previous studies, the presence of $InsP_7$ and $InsP_8$ is likely central for P_i
205 sensing in cells, as they promote the interaction of PHR with SPX proteins[10, 14, 15].
206 Intriguingly, our elemental analysis revealed that total P_i levels in shoots were not altered to
207 the same degree in *vih2-4*, although previous HPLC analyses of [^{3}H]-inositol-labeled
208 seedlings indicated that $InsP_8$ levels are strongly decreased in this mutant[17]. We further
209 confirmed by PAGE the strong decrease of $InsP_8$ in shoots of P_i-resupplied *vih2-4* plants (Fig.
210 3a and 3b). PAGE analysis also detected a significant increase in $InsP_7$ levels in *vih2-4* shoots
211 after P_i resupply (Fig. 3a and 3b), suggesting that a certain $InsP_7$ pool is regulated by VIH2-
212 dependent conversion to $InsP_8$ and that an increase of this pool in *vih2* mutant plants appears
213 to partially compensate for the loss of $InsP_8$ in regulating P_i signaling.

214 *ITPK1*, *VIH1* and *VIH2* are not only expressed in shoots but also in roots[13, 15]. However, since
215 little to no $InsP_7$ and $InsP_8$ could be detected by PAGE in roots of Arabidopsis and rice plants
216 (Fig. 2e and Suppl. Fig. 6), we wondered whether the availability of cytosolic $InsP_6$ could
217 determine the amount of $InsP_7$ and $InsP_8$ that can be synthesized. To test this hypothesis, we
218 assessed these PP-InsPs in shoots and roots of *mrp5*, a mutant defective in vacuolar loading of
219 $InsP_6$ [26]. In contrast to WT, we could detect $InsP_7$ and $InsP_8$ both in shoots and in roots of

mrp5 plants (Fig. 3c and 3d). Lack of *MRP5* resulted in higher levels of $InsP_7$ and $InsP_8$ as compared to WT but $InsP_8$ was still clearly responsive to P_i starvation and P_i resupply in this mutant. However, increased levels of these PP-InsPs in roots did not significantly affect P_i accumulation in *mrp5* shoots (Fig. 1b). Altogether, these results demonstrate that P_i-dependent synthesis of $InsP_7$ and $InsP_8$ relies on stepwise phosphorylation reactions mediated by ITPK1 and VIHs, and on the cytosolic/nucleoplasmic availability of $InsP_6$.

ITPK1 has $InsP_6$ kinase and ATP synthase activities

Recently, we demonstrated that recombinant ITPK1 phosphorylates $InsP_6$ *in vitro* at position 5 thereby generating 5-$InsP_7$, which is the main $InsP_7$ isomer detected in seeds[20]. Considering that ITPK1 is required for the robust increase in $InsP_8$ when P_i-deficient plants are resupplied with P_i (Fig. 2c and 2d), we asked whether ITPK1 is able to function as an $InsP_7$ kinase. As shown in Suppl. Fig. 7a, neither of the natural occurring isomers, 1-$InsP_7$ and 5-$InsP_7$, appears to be a substrate for ITPK1 kinase activity suggesting that the ITPK1-dependent increase in $InsP_8$ after P_i resupply is caused by an increase in a rate limiting pool of $InsP_7$. To further investigate the enzymatic properties of ITPK1, we performed nuclear magnetic resonance (NMR) assays with the recombinant protein taking advantage of [$^{13}C_6$]-labelled $InsP_6$. First, $InsP_6$ kinase reaction conditions were analyzed with respect to magnesium ion (Mg^{2+}) concentration and temperature dependencies as well as to quenching efficiency by EDTA (Suppl. Fig. 7b-d). Using 2.5 mM ATP, optimal enzyme activity was observed with as little as 2.5 mM Mg^{2+} and conversion could be fully quenched by a surplus of EDTA exceeding the Mg^{2+} concentration by 1.36 mM. Even though the protein behaved well at 37°C and increased kinase activities were observed at this elevated temperature (Suppl. Fig. 7d), we decided to carry out subsequent experiments at 25°C to more closely reflect temperatures in unstressed plants. Subsequent kinetic analysis revealed that ITPK1 exhibits a surprisingly high K_M for

ATP of approximately 520 µM (Fig. 4a and 4b). Unlike VIHs, the kinase activity of ITPK1 was largely insensitive to P_i and was also not affected by the non-metabolizable P_i analog phosphite (Suppl. Fig. 8). When $InsP_5$ [2-OH] was presented as substrate to ITPK1, no conversion could be detected (Suppl. Fig. 7e), suggesting that ITPK1 has no IPK-like activity to generate $InsP_6$ from $InsP_5$ [2-OH]. Furthermore, in contrast to $InsP_6$ kinases of the IP6K/Kcs1 family, no activity was observed when 1-$InsP_7$ was used as a substrate (Suppl. Fig. 7f and 7g), thus confirming our PAGE analysis (Suppl. Fig. 7a).

The characterization of structurally and sequence-unrelated mammalian $InsP_6$ kinases of the IP6K family has demonstrated that these enzymes can shift their activities from kinase to ADP phosphotransferase at low ATP-to-ADP ratios[27, 28]. This prompted us to assess if also ITPK1 possesses such activity. *In vitro* reactions with unlabeled 5-$InsP_7$ and subsequent PAGE analyses revealed that ITPK1 indeed mediates 5-$InsP_7$ hydrolysis and that this activity only occurs in the presence of ADP (Fig. 4c). A similar activity using any other $InsP_7$ isomer as phosphoryl donor could not be detected (Fig. 4d), suggesting a high degree of substrate specificity not only for ITPK1-mediated kinase activity but also for the reverse reaction (i.e., $InsP_7$ dephosphorylation / ATP synthesis). To determine the kinetic parameters of this reaction, we subsequently incubated ITPK1 with [$^{13}C_6$]-labelled 5-$InsP_7$ in the presence of ADP and detected the formation of ATP and $InsP_6$ (Suppl. Fig. 9a and 9b). No ATP formation was detected when the enzyme was incubated without 5-$InsP_7$ (Suppl. Fig. 10c). Interestingly, the velocity of the reverse reaction was almost two times faster than the forward reaction, whereas the K_M for ADP and ATP was relatively similar for ITPK1 (Fig. 4b, 4e and 4f). Taken together, these results demonstrate that ITPK1-mediated $InsP_6$ kinase and ADP phosphotransferase activities are regulated by adenylate energy charge. In agreement with results obtained in agar plate-grown seedlings[15], we observed that ATP levels and ATP/ADP ratios dropped significantly in response to P_i deficiency in shoots of hydroponically-grown

WT plants but rapidly increased after P_i resupply (Suppl. Fig. 10). Thus, the P_i-dependent changes in energy status of plants may ultimately regulate the synthesis of $InsP_7$ by shifting the activity of ITPK1.

ITPK1 activity in shoots controls PHR1- and PHL1-regulated PSRs

To directly address whether ITPK1-dependent synthesis of PP-InsPs in shoots or roots is responsible for P_i accumulation, we performed grafting experiments. As expected, shoot P_i overaccumulation was also detected when roots and shoots of *itpk1* plants were self-grafted (Fig. 5a). However, shoot P_i was almost back to WT levels when Col-0 shoots were grafted onto *itpk1* roots, while remaining approximately 75% higher when *itpk1* shoots were grafted onto Col-0 roots (Fig. 5a). Shoot dry weight or shoot levels of other nutrients were not significantly altered by the different graft combinations (Suppl. Fig. 11). These results suggest that ITPK1 activity in shoots is more determinant for the regulation of PSR and P_i accumulation.

We then addressed the putative involvement of ITPK1 in P_i signaling by analyzing the genetic interaction between ITPK1 and the transcription factors PHR1 and PHL1, which together control most of the transcriptional responses induced by P_i starvation[2]. Shoot growth was not significantly altered in homozygous double or triple mutants as compared to single or double mutants (Fig. 5b and 5c). Although *phr1 itpk1* and *phr1 phl1 itpk1* plants still accumulated significantly more P_i than *phr1* and *phr1 phl1*, respectively, the relative increments were smaller than in the presence of functional PHR1 and PHL1 (Fig. 5d). In turn, the short-root phenotype caused by *ITPK1* mutation could not be restored by knocking out these transcription factors (Suppl. Fig. 12). While most P_i starvation-induced transcriptional

responses were also suppressed in the triple mutant, absence of ITPK1 maintained *PHT1;8* up-regulated in the *phr1 phl1* background (Fig. 5e) potentially suggesting a PHR1/PHL1-independent regulation of *PHT1;8* expression. Finally, PAGE analysis revealed that $InsP_8$ levels remained very low when these two transcriptional regulators were knocked out (Fig. 5f and 5g). In contrast, P_i resupply-induced $InsP_7$ accumulation was largely independent of PHR1 and PHL1. Collectively, these observations demonstrate that ITPK1-dependent PP-InsP synthesis in shoots is required for undisturbed coordination of systemic P_i signaling by PHR1 and PHL1.

P_i-dependent synthesis of PP-InsPs is conserved across species

Next, we assessed whether P_i-dependent regulation of $InsP_7$ and $InsP_8$ is evolutionarily conserved across species. Similar to Arabidopsis, we observed that both $InsP_7$ and $InsP_8$ levels decreased strongly in response to P_i-deficiency in shoots of hydroponically-grown rice plants and were quickly restored by refeeding plants with P_i (Fig. 6a and 6b). Notably, in this species, a clear $InsP_7$ signal could be observed as soon as 30 min after P_i resupply and appeared before substantial changes in $InsP_8$ could be detected by PAGE. We also detected increased accumulation of PP-InsPs in P_i-replete and P_i-refed gametophores of the moss *Physcomitrella patens* (Fig. 6c-6e), suggesting that P_i-dependent $InsP_7$ and $InsP_8$ synthesis is also conserved in non-vascular land plants.

Since we recently showed that purified recombinant human ITPK1 is also able to catalyze 5-$InsP_7$ synthesis[20], we assessed P_i-dependent synthesis of PP-InsPs in the human HCT116 cell line. We found that while $InsP_6$ levels remained largely unaffected by P_i conditions, both $InsP_7$ and $InsP_8$ decreased in cells after removing P_i from the culture and sharply increased again after P_i resupply (Fig. 6f). Altogether, these results indicate that P_i-dependent synthesis of $InsP_7$ and $InsP_8$ seems to be evolutionary conserved across a range of different multicellular species.

DISCUSSION

Previously, isothermal titration calorimetry experiments demonstrated that 5-$InsP_7$ interacted more strongly with SPX domains than P_i and that 5-$InsP_7$ concentrations as low as 20 µM can effectively promote the interaction of OsSPX4 with OsPHR2[10], suggesting that $InsP_7$ can affect P_i signaling. The finding that an *itpk1* mutant in Arabidopsis over-accumulates P_i and constitutively express P_i starvation-induced genes under sufficient P_i (Fig. 1b; Suppl. Figs. 2 and 4)[13] provided further evidence that ITPK1 function is required for proper regulation of P_i homeostasis. In this work, we demonstrate that $InsP_7$ and $InsP_8$ most closely mirror P_i levels in different organisms as they decrease in response to P_i deficiency and quickly increase after P_i resupply (Fig. 2a-2c; Fig. 6). In *A. thaliana*, we show that both $InsP_7$ and $InsP_8$ levels are compromised in shoots of *itpk1* plants, especially when P_i-deficient plants are resupplied with P_i (Fig. 2c and 2d). Since we detected only $InsP_6$ kinase but no $InsP_7$ kinase activity with purified recombinant ITPK1 (Fig. 4c; Suppl. Fig. 7a)[20], the decreased $InsP_8$ levels in *itpk1* plants likely resulted from the diminished 5-$InsP_7$ available for the subsequent phosphorylation at the C1 position by VIH1 and VIH2. Our results also indicate that ITPK1 can shift its activity and become an ADP phosphotransferase that specifically hydrolyses 5-$InsP_7$ when adenylate energy charges are low, such as in P_i-deficient cells (Fig. 4; Suppl. Fig. 10). Thus, our results with ITPK1 and those of Zhu et al.[15] with VIH1 and VIH2 provide a detailed view on how changes in cellular P_i status alter the activity of these enzymes to efficiently produce and eliminate the signaling molecules $InsP_7$ and $InsP_8$ in plants (Fig. 7).

Although both ITPK1 and ITPK2 possess $InsP_6$ kinase activity[20], PSR seems only disturbed in *itpk1* but not *itpk2* mutants (Fig. 1b)[13]. PP-InsPs are not significantly altered in *itpk2* seedlings (Suppl. Fig. 5a)[21], suggesting that ITPK1 can fully compensate for the loss of ITPK2.

Furthermore, since only *ITPK2* transcription is induced by P_i deficiency (Suppl. Fig. 13), it is likely that ITPK1 and ITPK2 play independent roles in P_i signaling. In a previous study, the putative role of $InsP_7$ in plant P_i signaling was excluded because HPLC analysis of [^{32}P]-P_i-labeled plants showed that $InsP_7$ levels were similarly compromised in *itpk1* and *itpk4* plants[13], whereas only *itpk1* displays obvious PSR defects (Fig. 1b)[13]. However, our PAGE analyses showed that $InsP_7$ and $InsP_8$ levels are not compromised in the *itpk4-1* mutant (Suppl. Fig. 5b and 5c). Therefore, a role for $InsP_7$ and/or $InsP_8$ cannot be excluded based on the comparison of *itpk1* and *itpk4-1*. Meanwhile, two recent studies raised compelling evidence that $InsP_8$ acts as a signaling molecule to regulate P_i homeostasis in Arabidopsis, as *vih1 vih2* double mutants exhibit constitutive up-regulation of PSI genes and strong P_i hyperaccumulation[14, 15]. Here, we show that a P_i-dependent accumulation of $InsP_8$ and $InsP_7$ appears to be conserved in land plants, including dicotyledonous and monocotyledonous vascular species as well as non-vascular species (Fig. 2a-2c; Fig. 6a-e). Of note, our PAGE results from independent experiments demonstrate that $InsP_8$ is more sensitive to P_i than $InsP_7$. However, $InsP_7$ levels were clearly reduced when plants were exposed to more prolonged periods of P_i starvation (Fig. 6a, 6b and 6e). Furthermore, we also found that not only $InsP_7$ but also $InsP_8$ is induced by P_i in human HCT116 cells (Fig. 6f). P_i-dependent regulation of $InsP_8$ in human cells has likely also an impact on P_i homeostasis, as this PP-InsP was recently shown to be functionally dominant over 5-$InsP_7$ and 1-$InsP_7$ in the regulation of the cellular P_i exporter protein Xenotropic and Polytropic Retrovirus Receptor 1 (XPR1)[29].

In Arabidopsis, $InsP_8$ levels are strongly reduced while $InsP_7$ significantly increased in the *vih1 vih2* double mutant[15], suggesting that $InsP_7$ itself plays only a relatively minor role in P_i signaling. However, considering the evidence for the involvement of $InsP_8$ in other cellular processes [17, 30, 31], it might well be that the severe growth defects of *vih1 vih2* plants[14, 15] are not solely related to disturbed P_i homeostasis. Here, we analyzed the *vih2-4* single mutant,

368 which grows similarly to the WT (Fig. 1a), and found that whereas $InsP_8$ levels in *vih2-4*
369 plants were as low as in *itpk1*, strong P_i overaccumulation was only observed for *itpk1* plants
370 (Fig. 1b; Fig. 3a and 3b). Since $InsP_8$ reduction in *vih2-4* plants is accompanied by increased
371 $InsP_7$ levels (Fig. 3a and 3b), it is likely that, under certain circumstances, $InsP_7$ may partially
372 compensate for the loss of $InsP_8$. Noteworthy, also $InsP_7$ is involved in other cellular
373 processes, such as auxin perception, as 5-$InsP_7$ can bind to the auxin receptor complex[21].
374 Importantly, the role of ITPK1 in auxin perception is largely independent of its function in P_i
375 homeostasis[21], suggesting that different tissue-specific $InsP_7$ pools may regulate diverse
376 signaling pathways. This assumption is supported by the fact that the auxin-associated short-
377 root phenotype of *itpk1* plants cannot be complemented with P_i nor attenuated by disrupting
378 PHR1 and PHL1 (Fig. 1e and 1f; Suppl. Figs. 3 and 12). However, to directly assess the
379 contribution of $InsP_7$ to different physiological processes, it would be necessary to develop a
380 strategy to specifically disrupt $InsP_7$ synthesis without altering $InsP_8$ levels.

381 The genetic analysis of *phr1 itpk1* and *phr1 phl1 itpk1* multiple mutants demonstrated that, in
382 the absence of PHRs, *ITPK1* mutation did not anymore mis-regulate the expression of P_i
383 starvation-induced genes nor result in uncontrolled P_i accumulation under sufficient P_i (Fig.
384 5d and 5e). These results place ITPK1 upstream of PHRs and further support that P_i-
385 dependent synthesis of $InsP_7$ by ITPK1 and of $InsP_8$ by VIHs is critical for undisturbed P_i
386 signaling in plants. Our grafting experiment further demonstrated that P_i overaccumulation in
387 *itpk1* was mainly due to missing ITPK1 activity in shoots rather than in roots (Fig. 5a), thus
388 pointing to a major role of PP-InsPs in P_i signaling in shoots. This result was somewhat
389 surprising, since *ITPK1*, *VIH1* and *VIH2* are expressed in shoots and roots[13, 15, 17]. However, in
390 line with earlier indications from [^{32}P]-P_i-labeling[13], our PAGE analyses also detected much
391 higher $InsP_7$ and $InsP_8$ levels in shoots than in roots of both Arabidopsis and rice plants (Fig.
392 2c and 2e; Suppl. Fig. 6). However, accumulation of these PP-InsPs in roots could be induced

by disturbing MRP5-mediated $InsP_6$ loading into the vacuole (Fig. 3d). Nonetheless, it remains unknown whether $InsP_6$ availability to ITPK1 in leaves is also regulated by P_i. Whereas ITPK1 is located both in the nucleus and in the cytoplasm[13], VIH1 and VIH2 are reported to display cytoplasmic localizations[15]. Given that SPXs act as receptors for PP-InsPs[10, 14, 32, 33, 34], ligand availability controls the interaction between SPXs and PHRs. To affect P_i signaling, PP-InsPs most likely have to cross the nuclear envelope, especially because SPX1, SPX2 and SPX3 are localized in the nucleus[4, 35]. Alternatively, they may also interact with proteins located in the cytoplasm, such as SPX4[36].

The emerging model is that in the presence of low levels of PP-InsPs ligands, as when plants suffer from P_i deficiency (Fig. 2a-2d; Fig 6a-6e), SPX receptors are unable to bind to PHRs. Consequently, these transcription factors are free to bind to the P1BS motifs present in the promoters of several P_i-responsive genes[1, 2]. Our findings that $InsP_7$ and $InsP_8$ levels quickly increase after P_i resupply in different plant species (Fig. 2a-2d; Fig. 6a-6e) provide insights into how this mechanism can be reversed once P_i-starved plants regain access to P_i. It is likely that the increased ligand levels shortly overlap with high abundance of SPX proteins, allowing for the formation of SPX - PHR complexes and the subsequent quick inhibition of PHR-dependent transcriptional responses.

Our PAGE analyses demonstrate that $InsP_7$ and $InsP_8$ levels dynamically reflect the P_i status in different organisms, indicating that PP-InsPs synthesis and degradation (or simply turnover) must be tightly controlled. P_i-dependent accumulation of $InsP_8$ has been proposed to rely on the bifunctional activity of the diphosphoinositol pentakisphosphate kinases VIH1 and VIH2[14, 15]. The relative kinase and phosphatase activities of this type of bifunctional enzymes can be shifted according to cellular ATP and P_i levels. Indeed, purified Vip1 from yeast exhibited kinase activity and, hence, increased $InsP_8$ synthesis at higher ATP concentrations, whereas at low ATP levels the protein functioned mainly as an $InsP_8$ phosphatase[15]. In this

418 context, the phosphatase activity of diphosphoinositol pentakisphosphate kinases is further
419 inhibited by P_i itself[15, 22]. However, unlike VIHs, ITPK1 does not harbor the bifunctional
420 kinase domain - phosphatase domain architecture but only the atypical 'ATP-grasp fold'
421 ATP-binding site. Here, we demonstrate with independent approaches that ITPK1-mediated
422 $InsP_6$ conversion to 5-$InsP_7$ depends on ATP availability (Fig. 4). Our NMR-based kinetic
423 assays also revealed that Arabidopsis ITPK1 has a high K_M of approximately 523 µM for
424 ATP (Fig. 4b), which is similar to the K_M recorded for mammalian IP6Ks[27, 28], suggesting that
425 ITPK1-dependent InsP synthesis will be compromised at low cellular adenylate energy
426 charge.

427 In metazoans and yeast, PP-InsPs act as energy sensors and metabolic messengers[37, 38], and
428 fluctuations in ATP levels have been shown to correlate with changes in intracellular
429 concentrations of $InsP_7$ [39]. In our conditions, we observed that, compared to P_i-deficient
430 plants, ATP levels and ATP/ADP ratios are significantly higher in plants grown continuously
431 with sufficient P_i or shortly after P_i is resupplied to P_i-deficient plants (Suppl. Fig. 10).
432 Previous reports have indeed shown that in plants, yeast and human cells ATP levels drop in
433 response to P_i starvation[15, 22, 40, 41]. Interestingly, we found that ITPK1 has also a high K_M for
434 ADP and, in the presence of this adenine nucleotide, converted 5-$InsP_7$ to $InsP_6$ generating
435 ATP in the process (Fig. 4c, 4d and 4e; Suppl. Fig. 9a). This activity is reminiscent of the
436 ATP synthase activity recorded for mammalian IP6K-type $InsP_6$ kinases[27, 28] and even for the
437 human diphosphoinositol pentakisphosphate kinase PPIP5K2[42]. Our kinetic analyses
438 demonstrated that the enzyme has comparable K_M values for ATP and ADP and similar V_{max}
439 values, i.e. similar efficiencies for the forward and reverse reactions (Fig. 4b and 4f),
440 suggesting that relative adenylate energy charge determines whether ITPK1 phosphorylates
441 $InsP_6$ or synthesizes ATP from 5-$InsP_7$. Consequently, ITPK1 activity would allow cells to,
442 for example, rapidly remove the signaling molecule $InsP_7$ in low P_i conditions, when ATP

levels and ATP/ADP ratios decrease. This type of deactivation of $InsP_7$/$InsP_8$ signaling could bypass the requirement for dedicated PP-InsP hydrolases which are likely to slow down quick dynamic changes in PP-InsPs to induce jasmonate-related responses during wound response or insect attack[17], or when P_i becomes suddenly available (Fig. 2a-2d; Fig. 6). While activation of the reverse reaction is unlikely to significantly alter global cellular ATP pools, localized ATP synthesis could quickly suppress $InsP_7$-mediated P_i signaling and, at the same time, might buffer the adenylate energy charge in the vicinity of ITPK1 under conditions of low energy or low P_i supply. Thus, adenylate charge-driven changes in the activities of ITPK1 and VIHs may represent one underlying mechanism by which the cellular P_i status is transduced into specific PP-InsPs levels to regulate downstream signaling events.

METHODS

Arabidopsis thaliana: plant materials and growth conditions

Seeds of *Arabidopsis thaliana* T-DNA insertion lines *itpk1* (SAIL_65_D03), *itpk2-2* (SAIL_1182_E03), *itpk3* (SALK_120653), *itpk4-1* (SAIL_33_G08), *ipk1-1* (SALK_065337C), *vih2-4* (GK-080A07), *mips1* (SALK_023626), *mips2* (SALK_031685), *mips3* (SALK_120131), *mrp5* (GK-068B10), *pho2-1* (EMS mutant described previously[43]) and *phr1* (SALK_067629) were obtained from The European Arabidopsis Stock Centre (http://arabidopsis.info/). The *phr1 phl1* double mutant used in this study was described previously[12]. To generate the *phr1 itpk1* double and the *phr1 phl1 itpk1* triple mutant, we crossed *itpk1* (-/-) with, respectively, *phr1* (-/-) and the homozygous *phr1 phl1* mutant. F2 and F3 plants were genotyped by PCR using the primers indicated in Suppl. Table 1 to identify homozygous lines. Transgenic lines expressing the genomic *ITPK1* fragment in the *itpk1* background were generated as described previously[21].

For sterile culture, Arabidopsis seeds were surface sterilized in 70% (v/v) ethanol and 0.05% (v/v) Triton X-100 for 15 min and washed twice with 96% (v/v) ethanol. Sterilized seeds were

sown onto modified half-strength Murashige and Skoog (MS) medium[44] containing 0.5% sucrose, 1 mM MES pH 5.5 and solidified with 1% (w/v) Difco agar (Becton Dickinson). After 7 days of preculture, seedlings were transferred to vertical plates containing fresh solid media supplemented with either sufficient P_i (625 µM P_i) or low P_i (5 µM P_i). Plants were grown under axenic conditions in a growth cabinet under the following regime: 10/14 h light/dark; light intensity 120 µmol m^{-2} s^{-1} (fluorescent lamps); temperature 22°C/18°C.

For hydroponic culture, Arabidopsis seeds were pre-cultured on rock wool moistened with tap water. After 1 week, tap water was replaced by half-strength nutrient solution containing 2 mM NH_4NO_3, 1 mM KH_2PO_4, 1 mM $MgSO_4$, 1 mM KCl, 250 µM K_2SO_4, 250 µM $CaCl_2$, 100 µM Na-Fe-EDTA, 30 µM H_3BO_3, 5 µM $MnSO_4$, 1 µM $ZnSO_4$, 1 µM $CuSO_4$ and 0.7 µM $NaMoO_4$ (pH adjusted to 5.8 by KOH). After 7 days, nutrient solution was changed to full-strength and replaced once a week (first 3 weeks), twice a week in the fourth week, and every 2 days in the following weeks. Aeration was provided to roots from the third week onwards. To induce P_i deficiency, KH_2PO_4 was replaced by KCl and P_i resupply was performed by refeeding P_i-starved plants with 1 mM KH_2PO_4 for 12 h. Plants were grown hydroponically in a growth chamber under the above-mentioned conditions except that the light intensity was 200 µmol photons m^{-2} s^{-1} and supplied by halogen lamps.

Phenotypic characterization in soil substrate was performed by germinating seeds directly in pots filled with peat-based substrate (Klasmann-Deilmann GmbH, Germany). The pots were placed inside a conditioned growth chamber with a 22°C/18°C and 16-h/8-h light/dark regime at a light intensity of 120 µmol photons m^{-2} s^{-1} supplied by fluorescent lamps. Plants were bottom watered at regular intervals. Seedlings were thinned after 1 week to leave only two plants per pot. Whole shoots or different plant parts were harvested as indicated in the legend of figures.

Cultivation of rice in hydroponics

494 Rice plants (cv. Nipponbare) were cultivated in hydroponics inside a glasshouse with natural
495 light supplemented with high pressure sodium vapor lamps to ensure a minimum light
496 intensity of 300 µmol m^{-2} s^{-1}, and 30°C/25°C day (16 h)/night (8 h) temperature. Seeds were
497 germinated in darkness at 20°C for 3 days and then transferred to meshes floating on a
498 solution containing 0.5 mM $CaCl_2$ and 10 µM Na-Fe-EDTA, which was exchanged every
499 third day. After 10 days, homogenous seedlings were transplanted into 60-L tanks filled with
500 half-strength nutrient solution[45]. Ten days later, the nutrient solution was changed to full-
501 strength and exchanged every 10 days. During the whole growing period, the pH value was
502 adjusted to 5.5 every second day. P_i starvation was imposed for 10 days before starting P_i
503 resupply.
504
505 **Cultivation of *Physcomitrella patens***
506 *Physcomitrella patens* was grown on Knop medium[46] solidified with 0.8% agar (A7921,
507 Sigma). Light was provided by fluorescent lamps (60 µmol m^{-2} s^{-1}) under a regime of 16 h
508 light and 8 h darkness at constant 20°C. P_i treatments were achieved by transferring pre-
509 cultivated plants to fresh Knop solid media containing 1.8 mM KH_2PO_4 (+P_i) or 1.8 mM KCl
510 (-P_i) for 30 days. At the end of Pi starvation period, part of the plants was resupplied with 1.8
511 mM KH_2PO_4 and harvested after 24 h or 96 h.
512
513 **Cultivation of HCT116 cells**
514 Mammalian cells were cultivated as described[23]. Briefly, HCT116 cells were grown in
515 DMEM media supplemented with 10% fetal bovine serum (FBS) and 0.45% glucose in a
516 humidified atmosphere with 5% CO_2. Phosphate starvation was induced with DMEM without
517 sodium phosphate supplemented with 10% dialyzed FBS. Cells were washed twice in the
518 phosphate-free medium before incubation with DMEM media with or without phosphate.
519 Analysis of InsPs from HCT116 cell lines was performed as previously described[23].

520

521 **Grafting experiment**

522 Seedlings to be grafted were germinated on plates containing half-strength MS (Duchefa),
523 0.04 mg L^{-1} 6-benzylaminopurine (Sigma), 0.02 mg L^{-1} indole acetic acid (Sigma), and 10 g
524 L^{-1} Difco agar (Becton Dickinson). Five-day-old seedlings were grafted on the plate by the
525 90-degree blunt end technique with an ultra-fine micro knife (Fine Scientific Tools, USA)
526 without collars. The grafted seedlings remained on the plate for 2 weeks to allow the
527 formation of the graft union. Successfully unified seedlings were transplanted directly to peat-
528 based soil and whole shoots harvested for elemental analysis 2 weeks later.

529

530 **RNA isolation and quantitative real-time PCR**

531 Root and shoots tissues were collected by excision and immediately frozen in liquid N_2. Total
532 RNA was extracted with RNeasy Plant Mini Kit (Macherey-Nagel GmbH & Co KG,
533 Germany). Quantitative reverse transcriptase PCR reactions were conducted with the
534 CFX384TM Real-Time System (Biorad, Germany) and the Go Taq qPCR Master Mix
535 SybrGreen I (Promega) using the primers listed in Supplementary Table 1. *UBQ2* was used as
536 reference gene to normalize relative expression levels of all tested genes. Relative expression
537 was calculated according to published instructions[47].

538

539 **Elemental analysis**

540 Whole shoots were dried at 65°C and digested in concentrated HNO_3 in
541 polytetrafluoroethylene tubes under pressurized system (UltraCLAVE IV, MLS). Elemental
542 analysis of plant samples from hydroponics or pot experiments was performed by inductively
543 coupled plasma optical emission spectrometry (ICP-OES; iCAP 700, Thermo Fisher
544 Scientific), whereas samples from agar plate-grown plants were analyzed by sector field high-

resolution inductively coupled plasma-mass spectrometry (HR-ICP-MS; ELEMENT 2, Thermo Fisher Scientific). Element standards were prepared from certified reference materials from CPI International.

Titanium dioxide bead extraction and PAGE

InsPs purification and analysis was performed based on a previously established protocol[23, 24, 25]. All steps until dilution were performed at 4°C. TiO_2 beads (Titanium (IV) oxide rutile, Sigma Aldrich) were weighted to 10 mg for each sample and washed once in water and once in 1 M perchloric acid (PA). Liquid N_2 frozen plant material was homogenized using a pestle and immediately resuspended in 800 µl ice-cold PA. Samples were kept on ice for 10 min with short intermediate vortexing, then centrifuged for 10 min at 20,000×*g* at 4°C using a refrigerated bench top centrifuge. The supernatants were transferred into fresh 1.5 mL tubes and centrifuged again for 10 min at 20,000×*g*. To absorb InsPs onto the beads the supernatants were resuspended in the pre-washed TiO_2 beads and rotated at 4°C for 30-60 min. Afterwards, beads were pelleted by centrifuging at 8000 *g* for 1 min and washed twice in PA. The supernatants were discarded. To elute inositol polyphosphates, beads were resuspended in 200 µl 10% ammonium hydroxide and then rotated 5 min at room temperature. After centrifuging, the supernatants were transferred into fresh 1.5-mL tubes. The elution process was repeated and the second supernatants were added to the first. Eluted samples were vacuum evaporated at 45°C to dry completely. InsPs were resuspended in 20 µL ultrapure water and separated by 33% polyacrylamide gel electrophoresis and visualized by Toluidine Blue staining, followed by 4′,6-diamidino-2-phenylindole (DAPI) staining.

ITPK1 *in vitro* kinase and ATP synthase assay

569 Recombinant *A. thaliana* ITPK1 was purified based on the previously established protocol[48].
570 The $InsP_6$ kinase assay was performed by incubating 10.17 µM enzyme in a reaction mixture
571 containing 5 mM $MgCl_2$, 20 mM HEPES (pH 7.5), 1 mM DTT, 5 mM phosphocreatine, 0.33
572 units creatine kinase, 12.5 mM ATP and 1 mM $InsP_6$ (Sichem) at 25°C for 6h. The ability of
573 the enzyme to hydrolyze 5-$InsP_7$ was assayed in a reaction mixture containing 3 µg enzyme,
574 2.5 mM $MgCl_2$, 50 mM NaCl, 20 mM HEPES (pH 6.8), 1 mM DTT, 1 mg/mL BSA, 8 mM
575 ADP and 1 mM 5-$InsP_7$ at 25°C for 6h. Reactions were separated by 33% polyacrylamide gel
576 electrophoresis and visualized by Toluidine Blue staining.

577

578 **NMR-based enzyme assays**

579 Full-length recombinant *A. thaliana* ITPK1 in H_2O was used in all assays. 0.2-0.8 µM of
580 ITPK1 was incubated in reaction buffer containing 20 mM HEPES pH* 7.0, 50 mM NaCl, 1
581 mM DTT, 5 mM creatine phosphate, 1 U/ml creatine kinase, 2.5 mM $MgCl_2$ (if not indicated
582 otherwise) and 175 µM of [$^{13}C_6$]$InsP_5$ [2-OH], [$^{13}C_6$]$InsP_6$, [$^{13}C_6$]5-$InsP_7$ or [$^{13}C_6$]1-$InsP_7$ in
583 D_2O. If not indicated otherwise, the reaction buffer also included 2.5 mM ATP or 2.5 mM
584 ADP.
585 For single time-point analysis of enzyme activity, 2.25-0.375 ng (0.2-0.3 µM) ITPK1 were
586 used. 150 µL reactions were incubated at 25°C (except when 37°C is specified), quenched
587 with 400 µl of 20 mM EDTA (pH* 6.0 in D_2O) and 11 µL of 5 M NaCl was added for
588 analysis. For real-time monitoring of enzyme activity, 36 ng (0.8 µM) ITPK1 were used. 600
589 µL reactions were maintained at 25°C in an NMR spectrometer and measured consecutively
590 with 85 sec spectra.
591 Samples were measured as previously described[49] on Bruker AV-III spectrometers (Bruker
592 Biospin, Rheinstetten, Germany) using cryogenically cooled 5 mm TCI-triple resonance
593 probe equipped with one-axis self-shielded gradients and operating at 600 MHz for proton

nuclei, 151 MHz for carbon nuclei, and 244 MHz for P nuclei. The software to control the spectrometer was topspin 3.5 pl6. Temperature was calibrated using d_4-methanol and the formula of Findeisen et al.[50].

InsPs extraction from seedlings and HPLC analyses

Seedlings were grown vertically on half-strength MS medium supplemented with 1 % sucrose and 7 g L^{-1} Phytagel (P8169, Sigma), pH 5.7 for 12 days (8 h light at 22°C, 16 h darkness at 20°C). Seedlings were transferred to 3 mL half-strength MS liquid media without sucrose and with 625 µM P_i (+P) or 5 µM P_i (-P). Seedlings were labeled by adding 30 µCi mL^{-1} of [^{3}H]-*myo*-inositol (30 to 80 Ci $mmol^{-1}$ and 1 mCi mL^{-1}; American Radiolabeled Chemicals) and further cultivated for 5 days. For P_i-resupply, 620 µM KH_2PO_4 was added to the media and the plants were grown for another 6 h before harvest. Afterwards seedlings were washed two times with ultrapure water, frozen in liquid N_2 and the InsPs were extracted as described previously (Azevedo and Saiardi, 2006). Inositol polyphosphates were resolved by strong anion exchange chromatography HPLC (using a partisphere SAX 4.63 x 125 mm column; HiChrom) at a flow rate of 0.5 mL min^{-1} with a gradient of the following buffers: buffer A (1 mM EDTA) and buffer B (1 mM EDTA and 1.3 M $(NH_4)_2HPO_4$, pH 3.8, with H_3PO_4). The gradient was as follows: 0-2 min, 0 % buffer B; 2-7 min, up to 10 % buffer B; 7-68 min, up to 84 % buffer B; 68-82 min, up to 100 % buffer B; 82-100 min, 100 % buffer B, 100-101 min, down to 0 % buffer B; 101-125 min, 0 % buffer B. Fractions were collected each minute, mixed with scintillation cocktail (Perkin-Elmer; ULTIMA-FLO AP), and analyzed by scintillation counting. To account for differences in fresh weight and extraction efficiencies between samples, values shown are normalized activities based on the total activity of each sample. 'Total' activities for normalization were calculated by counting fractions from 26 min ($InsP_3$) until the end of the run.

620 **Analysis of ATP and ADP**

621 Adenosine nucleotides were specifically determined according to Haink and Deussen[51] with
622 some modifications. 100 mg frozen leaf material from Arabidopsis plants were homogenized
623 in liquid N_2 and extracted with methanol/chloroform[52]. An aliquot of extracted samples was
624 used for derivatization. Twenty µL of extract was added to 205 µL of a buffer containing 62
625 mM sodium citrate and 76 mM potassium dihydrogenphosphate for which pH was adjusted to
626 5.2 with potassium hydroxide. To this mixture, 25 µL chloracetaldehyde (Sigma-Aldrich,
627 Germany) was added and the whole solution was incubated for 40 min at 80°C followed by
628 cooling and centrifugation for 1 min at 14000 rpm. Two blanks containing all reagents except
629 plant extract were used as control. For quantification, external standards (ATP, ADP, AMP)
630 were established with different concentrations. Separation of adenosine nucleotides was
631 performed on a newly developed UPLC-based method using ultra pressure reversed phase
632 chromatography (Acquity H-Class, Waters GmbH, Eschborn, Germany). The UPLC system
633 consisted of a quaternary solvent manager, a sample manager-FTN, a column manager and a
634 fluorescent detector (PDA eλ Detector). The separation was carried out on a C18 reversed
635 phase column (YMC Triart, 1.9 µm, 2.0x100 mm ID, YMC Chromatography, Germany) with
636 a flow rate of 0.6 ml per min and duration of 7 min. The column was heated at 37°C during
637 the whole run. The detection wavelengths were 280 nm for excitation and 410 nm as
638 emission. The gradient was accomplished with two solutions. Eluent A was 5.7 mM
639 tetrabutylammonium bisulfate (TBAS) and 30.5 mM KH_2PO_4, pH adjusted to 5.8. Eluent B
640 was a mixture of pure acetonitrile and TBAS in a ratio of 2:1. The column was equilibrated
641 with eluent A (90%) and eluent B (10 %) for at least 30 minutes. The gradient was produced
642 as follow: 90% A and 10% B for 2 min, changed to 40% A and 60% B and kept for 2.3 min,
643 changed to 10% A and 90% B for 1.1 min and reversed to 90% A and 10% B for another 1.6
644 min.
645

646 **Statistical analysis**

647 To analyze the significant differences among multiple groups, one-way analysis of variance
648 followed by Tukey's test at $P < 0.05$ was adopted. The statistical significance between two
649 groups was assessed by two-tailed Student's *t*-test. All statistical tests were performed using
650 SigmaPlot 11.0 software.

651

652 # References

653 1. Rubio V, *et al.* A conserved MYB transcription factor involved in phosphate
654 starvation signaling both in vascular plants and in unicellular algae. *Gene Dev* **15**,
655 2122-2133 (2001).

656 2. Bustos R, *et al.* A central regulatory system largely controls transcriptional activation
657 and repression responses to phosphate starvation in Arabidopsis. *Plos Genet* **6**, -
658 (2010).

659 3. Lv QD, *et al.* SPX4 negatively regulates phosphate signaling and homeostasis through
660 its interaction with PHR2 in rice. *Plant Cell* **26**, 1586-1597 (2014).

661 4. Puga MI, *et al.* SPX1 is a phosphate-dependent inhibitor of PHOSPHATE
662 STARVATION RESPONSE 1 in Arabidopsis. *Proc Natl Acad Sci USA* **111**, 14947-
663 14952 (2014).

664 5. Wang ZY, *et al.* Rice SPX1 and SPX2 inhibit phosphate starvation responses through
665 interacting with PHR2 in a phosphate-dependent manner. *Proc Natl Acad Sci USA*
666 **111**, 14953-14958 (2014).

667 6. Qi WJ, Manfield IW, Muench SP, Baker A. AtSPX1 affects the AtPHR1-DNA-
668 binding equilibrium by binding monomeric AtPHR1 in solution. *Biochem J* **474**,
669 3675-3687 (2017).

670 7. Zhong Y, *et al.* Rice SPX6 negatively regulates the phosphate starvation response
671 through suppression of the transcription factor PHR2. *New Phytol* **219**, 135-148
672 (2018).

673 8. Liu F, *et al.* OsSPX1 suppresses the function of OsPHR2 in the regulation of
674 expression of OsPT2 and phosphate homeostasis in shoots of rice. *Plant J* **62**, 508-517
675 (2010).

676 9. Pratt J, Boisson AM, Gout E, Bligny R, Douce R, Aubert S. Phosphate (Pi) starvation
677 effect on the cytosolic pi concentration and pi exchanges across the tonoplast in plant
678 cells: An in vivo ^{31}P-nuclear magnetic resonance study using methylphosphonate as a
679 Pi analog. *Plant Physiol* **151**, 1646-1657 (2009).

680 10. Wild R, *et al.* Control of eukaryotic phosphate homeostasis by inositol polyphosphate
681 sensor domains. *Science* **352**, 986-990 (2016).

11. Stevenson-Paulik J, Bastidas RJ, Chiou ST, Frye RA, York JD. Generation of phytate-free seeds in Arabidopsis through disruption of inositol polyphosphate kinases. *Proc Natl Acad Sci USA* **102**, 12612-12617 (2005).

12. Kuo HF, Chang TY, Chiang SF, Wang WD, Charng YY, Chiou TJ. Arabidopsis inositol pentakisphosphate 2-kinase, AtIPK1, is required for growth and modulates phosphate homeostasis at the transcriptional level. *Plant J* **80**, 503-515 (2014).

13. Kuo HF, *et al.* Arabidopsis inositol phosphate kinases IPK1 and ITPK1 constitute a metabolic pathway in maintaining phosphate homeostasis. *Plant J* **95**, 613-630 (2018).

14. Dong J, *et al.* Inositol pyrophosphate InsP8 acts as an intracellular phosphate signal in Arabidopsis. *Mol Plant* **12**, 1463-1473 (2019).

15. Zhu J, *et al.* Two bifunctional inositol pyrophosphate kinases/phosphatases control plant phosphate homeostasis. *eLife* **8**, (2019).

16. Lonetti A, Szijgyarto Z, Bosch D, Loss O, Azevedo C, Saiardi A. Identification of an evolutionarily conserved family of inorganic polyphosphate endopolyphosphatases. *J Biol Chem* **286**, 31966-31974 (2011).

17. Laha D, *et al.* VIH2 regulates the synthesis of inositol pyrophosphate InsP8 and jasmonate-dependent defenses in Arabidopsis. *Plant Cell* **27**, 1082-1097 (2015).

18. Desai M, *et al.* Two inositol hexakisphosphate kinases drive inositol pyrophosphate synthesis in plants. *Plant J* **80**, 642-653 (2014).

19. Dollins DE, *et al.* Vip1 is a kinase and pyrophosphatase switch that regulates inositol diphosphate signaling. *Proc Natl Acad Sci USA*, 201908875 (2020).

20. Laha D, *et al.* Arabidopsis ITPK1 and ITPK2 have an evolutionarily conserved phytic acid kinase activity. *ACS Chem Biol* **14**, 2127-2133 (2019).

21. Laha NP, *et al.* ITPK1-dependent inositol polyphosphates regulate auxin responses in *Arabidopsis thaliana*. *bioRxiv*, 2020.2004.2023.058487 (2020).

22. Gu C, *et al.* The significance of the bifunctional kinase/phosphatase activities of diphosphoinositol pentakisphosphate kinases (PPIP5Ks) for coupling inositol pyrophosphate cell signaling to cellular phosphate homeostasis. *J Biol Chem* **292**, 4544-4555 (2017).

23. Wilson MSC, Bulley SJ, Pisani F, Irvine RF, Saiardi A. A novel method for the purification of inositol phosphates from biological samples reveals that no phytate is present in human plasma or urine. *Open Biol* **5**, (2015).

24. Losito O, Szijgyarto Z, Resnick AC, Saiardi A. Inositol pyrophosphates and their unique metabolic complexity: analysis by gel electrophoresis. *Plos One* **4**, (2009).

25. Wilson MS, Saiardi A. Inositol phosphates purification using titanium dioxide beads. *Bio Protoc* **8**, (2018).

26. Nagy R, *et al.* The Arabidopsis ATP-binding cassette protein AtMRP5/AtABCC5 is a high affinity inositol hexakisphosphate transporter involved in guard cell signaling and phytate storage. *J Biol Chem* **284**, 33614-33622 (2009).

27. Voglmaier SM, *et al.* Purified inositol hexakisphosphate kinase is an ATP synthase: diphosphoinositol pentakisphosphate as a high-energy phosphate donor. *Proc Natl Acad Sci U S A* **93**, 4305-4310 (1996).

28. Wundenberg T, Grabinski N, Lin HY, Mayr GW. Discovery of $InsP_6$-kinases as $InsP_6$-dephosphorylating enzymes provides a new mechanism of cytosolic $InsP_6$ degradation driven by the cellular ATP/ADP ratio. *Biochem J* **462**, 173-184 (2014).

29. Li X, *et al.* Control of XPR1-dependent cellular phosphate efflux by $InsP_8$ is an exemplar for functionally-exclusive inositol pyrophosphate signaling. *Proc Natl Acad Sci U S A* **117**, 3568-3574 (2020).

30. Couso I, *et al.* Synergism between inositol polyphosphates and TOR kinase signaling in nutrient sensing, growth control, and lipid metabolism in Chlamydomonas. *Plant Cell* **28**, 2026-2042 (2016).

31. Laha D, *et al.* Inositol polyphosphate binding specificity of the jasmonate receptor complex. *Plant Physiol* **171**, 2364-2370 (2016).

32. Wilson MS, Jessen HJ, Saiardi A. The inositol hexakisphosphate kinases IP6K1 and -2 regulate human cellular phosphate homeostasis, including XPR1-mediated phosphate export. *J Biol Chem* **294**, 11597-11608 (2019).

33. Ried MK, *et al.* Inositol pyrophosphates promote the interaction of SPX domains with the coiled-coil motif of PHR transcription factors to regulate plant phosphate homeostasis. *bioRxiv*, 2019.2012.2013.875393 (2019).

34. Azevedo C, Saiardi A. Eukaryotic phosphate homeostasis: The inositol pyrophosphate perspective. *Trends Biochem Sci* **42**, 219-231 (2017).

35. Duan K, Yi KK, Dang L, Huang HJ, Wu W, Wu P. Characterization of a sub-family of Arabidopsis genes with the SPX domain reveals their diverse functions in plant tolerance to phosphorus starvation. *Plant J* **54**, 965-975 (2008).

36. Osorio MB, *et al.* SPX4 acts on PHR1-dependent and -independent regulation of shoot phosphorus status in Arabidopsis. *Plant Physiol* **181**, 332-352 (2019).

37. Shears SB. Diphosphoinositol polyphosphates: metabolic messengers? *Mol Pharmacol* **76**, 236-252 (2009).

38. Wilson MSC, Livermore TM, Saiardi A. Inositol pyrophosphates: between signalling and metabolism. *Biochem J* **452**, 369-379 (2013).

39. Szijgyarto Z, Garedew A, Azevedo C, Saiardi A. Influence of inositol pyrophosphates on cellular energy dynamics. *Science* **334**, 802-805 (2011).

40. Choi J, Rajagopal A, Xu YF, Rabinowitz JD, O'Shea EK. A systematic genetic screen for genes involved in sensing inorganic phosphate availability in *Saccharomyces cerevisiae*. *Plos One* **12**, (2017).

41. Desfougeres Y, Wilson MSC, Laha D, Miller GJ, Saiardi A. ITPK1 mediates the lipid-independent synthesis of inositol phosphates controlled by metabolism. *Proc Natl Acad Sci U S A* **116**, 24551-24561 (2019).

42. An Y, Jessen HJ, Wang H, Shears SB, Kireev D. Dynamics of substrate processing by PPIP5K2, a versatile catalytic machine. *Structure* **27**, 1022-1028 e1022 (2019).

43. Delhaize E, Randall PJ. Characterization of a phosphate-accumulator mutant of *Arabidopsis thaliana*. *Plant Physiol* **107**, 207-213 (1995).

44. Gruber BD, Giehl RFH, Friedel S, von Wirén N. Plasticity of the *Arabidopsis* root system under nutrient deficiencies. *Plant Physiol* **163**, 161-179 (2013).

45. Yoshida S. *Laboratory manual for physiological studies of rice*. IRRI (1976).

46. Reski R, Abel WO. Induction of budding on chloronemata and caulonemata of the moss, Physcomitrella patens, using isopentenyladenine. *Planta* **165**, 354-358 (1985).

47. Pfaffl MW. A new mathematical model for relative quantification in real-time RT-PCR. *Nucleic Acids Res* **29**, e45 (2001).

48. Schaaf G, Betts L, Garrett TA, Raetz CR, Bankaitis VA. Crystallization and preliminary X-ray diffraction analysis of phospholipid-bound Sfh1p, a member of the Saccharomyces cerevisiae Sec14p-like phosphatidylinositol transfer protein family. *Acta Crystallogr Sect F Struct Biol Cryst Commun* **62**, 1156-1160 (2006).

49. Harmel RK, Puschmann R, Nguyen Trung M, Saiardi A, Schmieder P, Fiedler D. Harnessing ^{13}C-labeled myo-inositol to interrogate inositol phosphate messengers by NMR. *Chem Sci* **10**, 5267-5274 (2019).

50. Findeisen M, Brand T, Berger S. A ^{1}H-NMR thermometer suitable for cryoprobes. *Magn Reson Chem* **45**, 175-178 (2007).

51. Haink G, Deussen A. Liquid chromatography method for the analysis of adenosine compounds. *J Chromatogr B Analyt Technol Biomed Life Sci* **784**, 189-193 (2003).

52. Ghaffari MR, *et al.* The metabolic signature of biomass formation in barley. *Plant Cell Physiol* **57**, 1943-1960 (2016).

Acknowledgments

This work was funded by grants from the Deutsche Forschungsgemeinschaft (DFG, German Research Council) (HE 8362/1-1 to R.F.H.G.; SCHA 1274/4-1, SCHA 1274/5-1, Research Training Group GRK 2064 and under Germany's Excellence Strategy, EXC-2070-390732324, PhenoRob to G.S.; CIBSS – EXC 2189 – 390939984 as well as JE 572/4-1 to H.J.J.; and LA 4541/1-1, Postdoctoral Research Fellowship, to D.L.) and from the Medical Research Council (MRC) MC_UU_00012/4 to A.S. We thank Annett Bieber, Jacqueline Fuge, Nicole Schäfer and Yudelsy A. Tandron Moya (Leibniz Institute of Plant Genetics and

Crop Plant Research) for excellent technical assistance, and Nicolaus von Wirén for critically reading the article. We thank Saikat Bhattacharjee (RCB, India) for providing seeds of published *Arabidopsis thaliana* mutants.

Author contributions

G.S. and R.F.H.G. conceived the study. D.L., R.K.H., M.F., G.S., and R.F.H.G. designed experiments. E.R., D.L., R.K.H., P.G., V.P., M.F., N.P.L., L.K., R.S., and R.F.H.G. performed experiments. M.-R.H. performed UPLC analysis of ATP and ADP. H.J.J. synthesized various InsP isomers. A.S., D.F., G.S., and R.F.H.G. supervised experimental work. R.F.H.G. and G.S. wrote the manuscript with critical inputs from all authors.

Conflict of interest

Conflicts of interest: No conflicts of interest declared.

Figure legends

Fig. 1. Role of distinct InsP kinases in plant P_i accumulation.

a-b Photographs of 3-week-old *Arabidopsis* plants grown on peat-substrate (**a**), and total P_i levels in shoots (**b**) of WT (Col-0) and the indicated mutants. Data represent means ± SD (*n* = 6-9 plants). Scale bars = 2 cm. **c-d** *ITPK1* expression (**c**) and shoot P_i levels (**d**) in 3-week-old WT (Col-0), *itpk1* and three independent *itpk1* lines transformed with *ITPK1* genomic DNA. Data represent means ± SD (*n* = 3 biological replicates in **c** and *n* = 8-9 plants in **d**). **e-h** Loss of ITPK1 results in P_i overaccumulation only in shoots but P_i-independent root growth repression. Phenotypes (**e**), primary root length (**f**) and total P_i concentrations in shoots (**g**) or roots (**h**) of plants grown in agar plates with sufficient (625 μM P_i) or deficient P_i supply (5

µM P_i) for 7 days. Bars show means ± SD (*n* = 6 replicates with 3 plants each). Different letters indicate significant differences according to Tukey's test ($P < 0.05$).

Fig. 2. $InsP_7$ and $InsP_8$ levels in shoots respond to P_i availability in an ITPK1-dependent manner.

a-b HPLC profiles of 17-day-old *Arabidopsis* WT (Col-0) seedlings radiolabeled with [^{3}H]-*myo*-inositol. Seedlings were grown either with P_i (+P) or without P_i (-P) or resupplied with P_i for 6 h prior to harvest (Pi RS 6h). Full, normalized spectra (**a**) and zoom-in view of the same profile (**b**). The experiment was repeated two times with similar results, and representative results from one experiment are shown. **c-e** PAGE of InsP levels in shoots (**c**), quantification of PAGE signals from shoots (**d**) and PAGE of roots (**e**) of WT (Col-0) and *itpk1* plants. Plants were grown in hydroponics in P_i-sufficient solution (+P), exposed for 4 days to P_i starvation (-P) or resupplied with P_i for 12 hours (Pi RS 12h). InsPs were eluted from TiO_2 beads, separated by PAGE and visualized by Toluidine blue and DAPI. Data represent means ± SE (n = 3-4 biological replicates). *$P < 0.05$, **$P < 0.01$ and ***$P < 0.001$ according to pairwise comparison with Student's *t*-test. **f-g** $InsP_7$ and $InsP_8$ levels are strongly increased in the shoots of the P_i-overaccumulating mutant *pho2-1*. PAGE of shoots (**f**) and shoot P_i levels in response to P_i deficiency and P_i resupply (**g**). Plants were cultivated as described in **c-e**. Data represent means ± SE (*n* = 4). Different letters indicate significant differences according to Tukey's test ($P < 0.05$).

Fig. 3. ITPK1- and VIH2-dependent synthesis of PP-InsPs and dependency on $InsP_6$ compartmentation.

a-b Loss of VIH2 increases $InsP_7$ levels in shoots. InsP detection in shoots of *Arabidopsis* WT, *itpk1* and *vih2-4* plants (**a**) and quantification of PAGE signals (**b**) 12 h after P_i resupply to P_i-starved plants in hydroponics. Data represent means ± SE (*n* = 4 biological replicates).

842 *$P < 0.05$, **$P < 0.01$ and ***$P < 0.001$ according to pairwise comparison with Student's *t*-
843 test. **c-d** Impaired $InsP_6$ transport into the vacuole increases $InsP_7$ and $InsP_8$ levels in shoots
844 and roots. InsP determination in shoots (**c**) and roots (**d**) of WT (Col-0) and *mrp5*. Plants were
845 grown in hydroponics in P_i -sufficient solution (+P), exposed for 4 days to P_i starvation (-P) or
846 resupplied with P_i for 12 hours (Pi RS 12h).
847
848 **Fig. 4. *In vitro* characterization of ITPK1 activity.**
849 **a-b** NMR analysis of InsP6 kinase activity of recombinant *Arabidopsis* ITPK1. Time-
850 dependent conversion of $InsP_6$ to 5-$InsP_7$ (**a**) and reaction velocity determined at varying ATP
851 concentrations (**b**). K_M and V_{max} were obtained after fitting of the data against the Michaelis-
852 Menten model. **c-d** In the presence of ADP, recombinant *Arabidopsis* ITPK1 mediates 5-
853 $InsP_7$ hydrolysis (**c**) but not the hydrolysis of other $InsP_7$ isomers (**d**). InsPs were separated via
854 PAGE and visualized by Toluidine Blue staining. The identity of bands was determined by
855 migration compared to $InsP_6$ and 5-$InsP_7$ standards and TiO_2-purified *mrp5* seed extract. $InsP_6$
856 kinase reaction served as positive control for the reverse reactions. Purified His_8-MBP tag
857 (MBP) served as negative control for ITPK1. Arrowhead in **c**, indicates the presence of a
858 small ATP band just above ADP. **e-f** NMR analysis of reverse reaction of recombinant
859 *Arabidopsis* ITPK1. Accumulation of $InsP_6$ and conversion of 5-$InsP_7$ (**e**) and reaction
860 velocity determined at varying ADP concentrations (**f**). K_M and V_{max} were obtained after
861 fitting of the data against the Michaelis-Menten model.
862
863 **Fig. 5. P_i starvation responses are mainly regulated by ITPK1 activity in shoots.**
864 **a** Total P_i concentration in shoots of self-grafted or reciprocally grafted WT (Col-0) and *itpk1*.
865 Plants were grafted on agar plates and left recovering for 2 weeks. Positive grafts were
866 transferred to peat-based substrate for another 2 weeks. Data represent means ± SD (*n* = 5-7
867 plants). **b-d** Genetic interplay between PHR1/PHL1 and ITPK1 in P_i sensing. Phenotype (**b**),

868 shoot dry weight (**c**) and shoot P_i levels (**d**) of 3-week-old WT and indicated mutants grown
869 on peat-based substrate. Data represent means ± SD (*n* = 6 plants). In **a**, **c** and **d**, letters
870 indicate significant differences according to Tukey's test ($P < 0.05$). **e** ITPK1-dependent
871 expression of P_i deficiency-induced genes in roots of the indicated P_i-sufficient plants. Data
872 represent means ± SE (*n* = 4 replicates). **f-g** PHR1- and PHL1-dependent synthesis of InsPs as
873 revealed by PAGE (**f**) and relative quantification of signals (**g**) in indicated double and triple
874 mutants grown in hydroponics with P_i-sufficient solution (+P), exposed to 4 days of P_i
875 starvation (-P) or resupplied with P_i for 12 hours (Pi RS 12h). Data represent means ± SE (*n* =
876 4 biological replicates). $*P < 0.05$, $**P < 0.01$ and $***P < 0.001$ according to pairwise
877 comparison with Student's *t*-test.
878
879 **Fig. 6. P_i-dependent regulation of $InsP_8$ levels is conserved in multicellular organisms.**
880 **a-b** Time-course analysis of InsPs in response to P_i starvation and P_i resupply in rice shoots.
881 PAGE (**a**) and relative quantification of bands (**b**) of rice plants cv. Nipponbare grown in
882 hydroponics. Data represent means ± SE (*n* = 4 biological replicates). Different letters
883 indicate significant differences according to Tukey's test ($P < 0.05$). **c-e** Phenotype (**c**), total
884 P_i levels (**d**) and PAGE of P_i-dependent synthesis of $InsP_7$ and $InsP_8$ (**e**) in gametophores of
885 *Physcomitrella patens*. Plants were cultivated on sufficient P_i (+P), starved of P_i for 30 days (-
886 P) or resupplied with P_i for the indicated time. Data represent means ± SD (*n* = 3 biological
887 replicates). Different letters indicate significant differences according to Tukey's test ($P <$
888 0.05). **f** PAGE analysis of wild-type HCT116 cell extracts during P_i starvation and resupply.
889 Cells were starved in P_i-free media for 18 h and resupplied with P_i for 3.5 h. Cells were
890 harvested at the same time. The experiment was repeated twice with similar results.
891
892 **Fig. 7. Model for ITPK1-dependent generation and removal of $InsP_7$ and its link with**
893 **VIHs and P_i signaling.**

In P_i-deficient cells, low ATP levels stimulate ITPK1 to catalyze P_i transfer from $InsP_7$ to ADP, thereby generating ATP and decreasing $InsP_7$. Decreased ATP and P_i levels also activate the pyrophosphatase activity of VIHs to break down $InsP_8$. The removal of PP-InsPs destabilizes the association between PHRs and SPXs, allowing PHRs to induce P_i starvation responses. When cells regain sufficient P_i, which increase ATP levels, ITPK1-mediated $InsP_6$ kinase activity is stimulated and the reverse reaction towards $InsP_7$ is inhibited. $InsP_7$ generated by ITPK1 serves then as substrate for $InsP_8$ production via the kinase domain of VIHs. As a consequence of increased PP-InsPs, SPX proteins recruit PHRs to repress P_i starvation responses.

Supplementary Figure 1. Shoot elemental analysis of WT, *itpk1* and recomplemented lines.

Dry weight of whole shoots (**a**) and shoot concentrations of the macronutrients calcium (**b**), potassium (**c**), magnesium (**d**) and sulfur (**e**), and the micronutrients iron (**f**), and zinc (**g**) of 3-week-old plants grown on peat-substrate. Data represent the mean ± SD (n = 8-9 plants). Different letters indicate significant differences according to Tukey's test ($P < 0.05$).

Supplementary Figure 2. ITPK1-dependent P overaccumulation in different plant organs.

Total P_i levels in different parts of WT (Col-0) and *itpk1* plants grown on peat-based. Data represent means ± SD (n = samples from 5 independent plants). Letters indicate significant differences according to Tukey's test ($P < 0.05$). Young siliques = green siliques with a length of 0.8 cm to 1.5 cm.

Supplementary Figure 3. Root phenotype of *itpk1* plants grown in hydroponics and of *pho2-1* grown in agar.

a Phenotype of 5-week-old WT and *itpk1* plants grown in hydroponics with sufficient P_i. Representative plants are shown. **b** Phenotype of WT and *pho2-1* plants grown in agar plates. Seven-day-old seedlings germinated on half-strength solid MS agar media containing 625 µM P_i were transferred to +P (625 µM P_i) or -P (5 µM P_i) and grown for additional 7 days.

Supplementary Figure 4. Expression of PSI genes in *itpk1* plants under different P_i conditions.

Expression analysis of representative P_i starvation-induced genes in *itpk1* relative to WT (Col-0). In **a** and **b**, the expression of P_i uptake- and signaling-related genes is shown, respectively. Seven-day-old seedlings germinated on half-strength solid MS agar media containing 625 µM P_i were transferred to same agar media containing either sufficient (625 µM) or deficient (5 µM) P_i levels for 4 days. For P_i refeeding, P_i-deficient plants were transferred back to P_i-containing media for 6 hours. Data represents means ± SE (n = 4 biological replicates). * P < 0.05, ** P < 0.01 and *** P < 0.001 according to pairwise comparison with Student's t-test (*itpk1* versus Col-0).

Supplementary Figure 5. P_i-dependent $InsP_7$ and $InsP_8$ synthesis is not altered in *itpk2-2* and *itpk4-1* mutant.

InsP detection in shoots of WT and *itpk2-2* (**a**) and *itpk4-1* plants (**b**) and relative quantification of PAGE signals for *itpk4-1* (**c**). Plants were grown in hydroponics under sufficient P_i (+P), after 4 days of P_i deficiency (-P) or after resupply of P_i to P_i-deficient plants for 12 h (RS 12h). Data represent means ± SE (n = 3 biological replicates).

Supplementary Figure 6. P_i-dependent regulation of InsP levels in roots and shoots of rice plants.

PAGE analysis of rice plants cv. Nipponbare grown in hydroponics under the indicated P_i conditions. Shown are representative gels from root and shoot samples.

Supplementary Figure 7. ITPK1 activity on $InsP_5$ [2-OH] and $InsP_7$ isomers and control experiments for the kinase activity.

a ITPK1 has no kinase activity on InsP7 isormers. 1-$InsP_7$, 5-$InsP_7$ or $InsP_6$ were incubated with recombinant *Arabidopsis* ITPK1 as indicated in presence of 12.5 mM ATP. InsPs were separated via PAGE and visualized by Toluidine Blue staining. The identity of bands was determined by migration compared to the substrates in absence of enzyme (-). Purified His_8-MBP tag (MBP) served as negative control for ITPK1. **b-d** Control experiments for NMR analyses. $InsP_6$ was incubated with recombinant *Arabidopsis* ITPK1 at 25 °C in the presence of 2.5 mM ATP. Enzymatic activity was determined after 24 h in the presence of varying EDTA concentrations (**b**), after 1.5 h at changing Mg^{2+} concentrations (**c**) and temperature (**d**). The conversion was determined by NMR spectroscopy after quenching with an excess of EDTA. **e-f** 2D ^{1}H-^{13}C-HMBC spectra. Recombinant *Arabidopsis* ITPK1 was incubated with $InsP_5$ (**e**) or 1-$InsP_7$ (**f**) at 25°C in the presence of an ATP recycling system for 24 h. The reaction mixture analyzed by HSQC NMR spectroscopy. **g** Overview of the reaction shown in (**f**) as analyzed by ^{31}P NMR spectroscopy after 24 h. A small, unidentified signal potentially reflecting ATP is marked with a question mark.

Supplementary Figure 8. Dependency of ITPK1 kinase activity on P_i.

$InsP_6$ was incubated with recombinant *Arabidopsis* ITPK1 at 25°C in the presence of 2.5 mM ATP and the indicated concentrations of P_i or its non-metabolizable analog phosphite (Phi).

968 The conversion was determined by NMR spectroscopy after quenching with an excess of
969 EDTA. The experiment was repeated three times.
970
971 **Supplementary Figure 9. Recombinant *Arabidopsis* ITPK1 can hydrolyze 5-InsP$_7$ in the**
972 **presence of ADP.**
973 **a** ^{31}P NMR spectroscopy analysis of recombinant *Arabidopsis* ITPK1 incubated with 5-InsP$_7$
974 at 25°C in the presence of ADP. After 24 h the mixture was analyzed by. **b** ^{31}P NMR analysis
975 of ATP in ATP synthase reaction buffer. **c** ^{31}P NMR spectroscopy analysis of recombinant
976 *Arabidopsis* ITPK1 incubated with ADP without 5-InsP$_7$ at 25°C and analyzed after 24 h. A
977 small, unidentified signal potentially reflecting ATP is marked with a question mark.
978
979 **Supplementary Figure 10. Effect of P$_i$ availability and resupply on shoot ATP levels.**
980 Concentration of ATP (**a**) and ATP/ADP ratios (**b**) in shoots of Col-0 plants grown in
981 hydroponics with P$_i$-sufficient solution (+P), exposed to 4 days of P$_i$ starvation (-P) or
982 resupplied with P$_i$ for 12 hours (Pi RS 12h). Data represent means ± SE (n = 6–7 biological
983 replicates). * $P < 0.05$ and ** $P < 0.01$ for the indicated pairwise comparisons with Student's
984 *t*-test.
985
986 **Supplementary Figure 11. Shoot ITPK1 function is more determinant for P$_i$**
987 **accumulation in plants.**
988 Shoot dry weight and shoot concentrations of the macronutrients potassium (K), calcium (Ca),
989 magnesium (Mg) and the micronutrient iron (Fe) of self-grafted or reciprocally grafted WT
990 (Col-0) and *itpk1*. Plants were grafted on agar plates and left recovering for 2 weeks. Positive
991 grafts were transferred to peat-based substrate for another 2 weeks. Data represent means ±
992 SD (n = 5-7 plants). Different letters indicate significant differences according to Tukey's test
993 ($P < 0.05$). n.s., not significant.

Supplementary Figure 12. ITPK1-dependent root phenotype in the absence of PHR1 and PHL1.

Seven-day-old seedlings germinated on half-strength solid MS agar media containing 625 µM P_i were transferred to +P (625 µM P_i) and grown for additional 7 days. Shown are representative images of the indicated mutants grown side-by-side on the same agar plate.

Supplementary Figure 13. P_i-dependent transcriptional regulation of InsP-related genes in Col-0 roots.

Seven-day-old Col-0 seedlings germinated on half-strength solid MS agar media were transferred to the indicated treatments for 4 days. +P, 625 µM P_i; -P, 5 µM P_i; Pi RS, P_i-starved plants were transferred back to P_i-containing media for 6 hours. Data represent mean ± SE (*n* = 3 biological replicates).

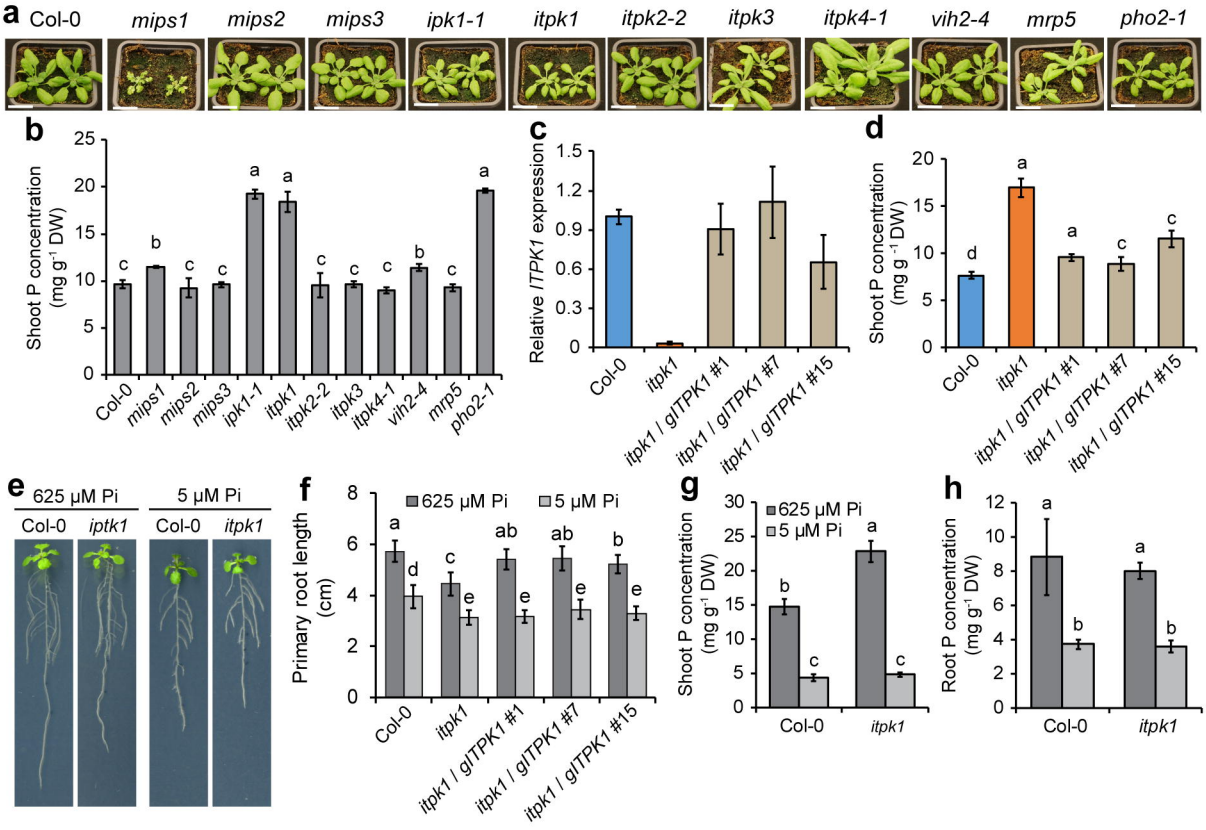

Fig. 1. Role of distinct InsP kinases in plant P_i accumulation.

a-b Photographs of 3-week-old *Arabidopsis* plants grown on peat-substrate (**a**), and total P_i levels in shoots (**b**) of WT (Col-0) and the indicated mutants. Data represent means ± SD (n = 6-9 plants). Scale bars = 2 cm. **c-d** *ITPK1* expression (**c**) and shoot P_i levels (**d**) in 3-week-old WT (Col-0), *itpk1* and three independent *itpk1* lines transformed with *ITPK1* genomic DNA. Data represent means ± SD (n = 3 biological replicates in **c** and n = 8-9 plants in **d**). **e-h** Loss of ITPK1 results in P_i overaccumulation only in shoots but P_i-independent root growth repression. Phenotypes (**e**), primary root length (**f**) and total P_i concentrations in shoots (**g**) or roots (**h**) of plants grown in agar plates with sufficient (625 µM P_i) or deficient P_i supply (5 µM P_i) for 7 days. Bars show means ± SD (n = 6 replicates with 3 plants each). Different letters indicate significant differences according to Tukey's test ($P < 0.05$).

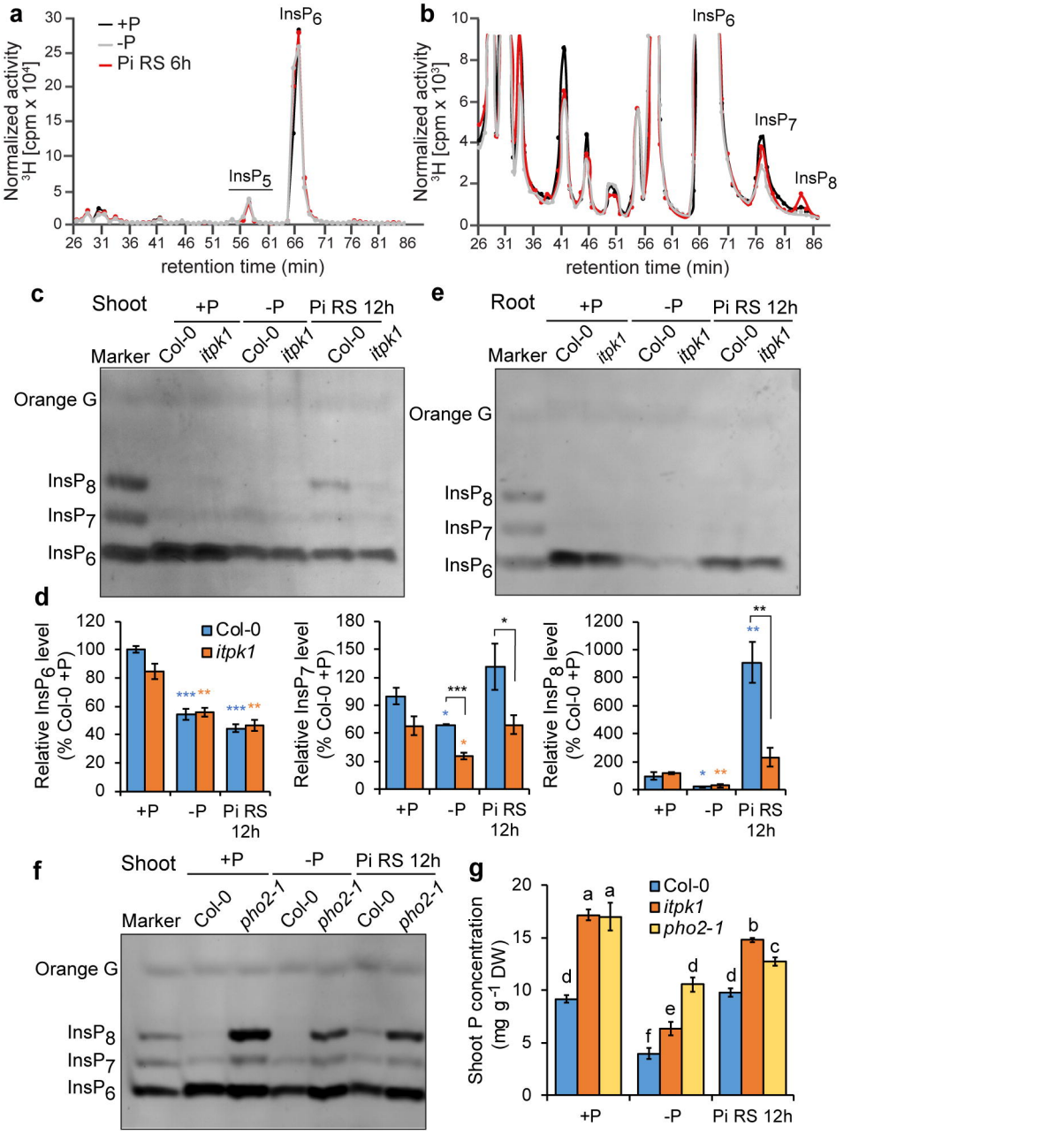

Fig. 2. $InsP_7$ and $InsP_8$ levels in shoots respond to P_i availability in an ITPK1-dependent manner.

a-b HPLC profiles of 17-day-old *Arabidopsis* WT (Col-0) seedlings radiolabeled with [^{3}H]-*myo*-inositol. Seedlings were grown either with P_i (+P) or without P_i (-P) or resupplied with P_i for 6 h prior to harvest (Pi RS 6h). Full, normalized spectra (**a**) and zoom-in view of the same profile (**b**). The experiment was repeated two times with similar results, and representative results from one experiment are shown. **c-e** PAGE of InsP levels in shoots (**c**), quantification of PAGE signals from shoots (**d**) and PAGE of roots (**e**) of WT (Col-0) and *itpk1* plants. Plants were grown in hydroponics in P_i-sufficient solution (+P), exposed for 4 days to P_i starvation (-P) or resupplied with P_i for 12 hours (Pi RS 12h). InsPs were eluted from TiO_2 beads, separated by PAGE and visualized by Toluidine blue and DAPI. Data represent means ± SE (n = 3-4 biological replicates). $*P < 0.05$, $**P < 0.01$ and $***P < 0.001$ according to pairwise comparison with Student's *t*-test. **f-g** $InsP_7$ and $InsP_8$ levels are strongly increased in the shoots of the P_i-overaccumulating mutant *pho2-1*. PAGE of shoots (**f**) and shoot P_i levels in response to P_i deficiency and P_i resupply (**g**). Plants were cultivated as described in **c-e**. Data represent means ± SE ($n = 4$). Different letters indicate significant differences according to Tukey's test ($P < 0.05$).

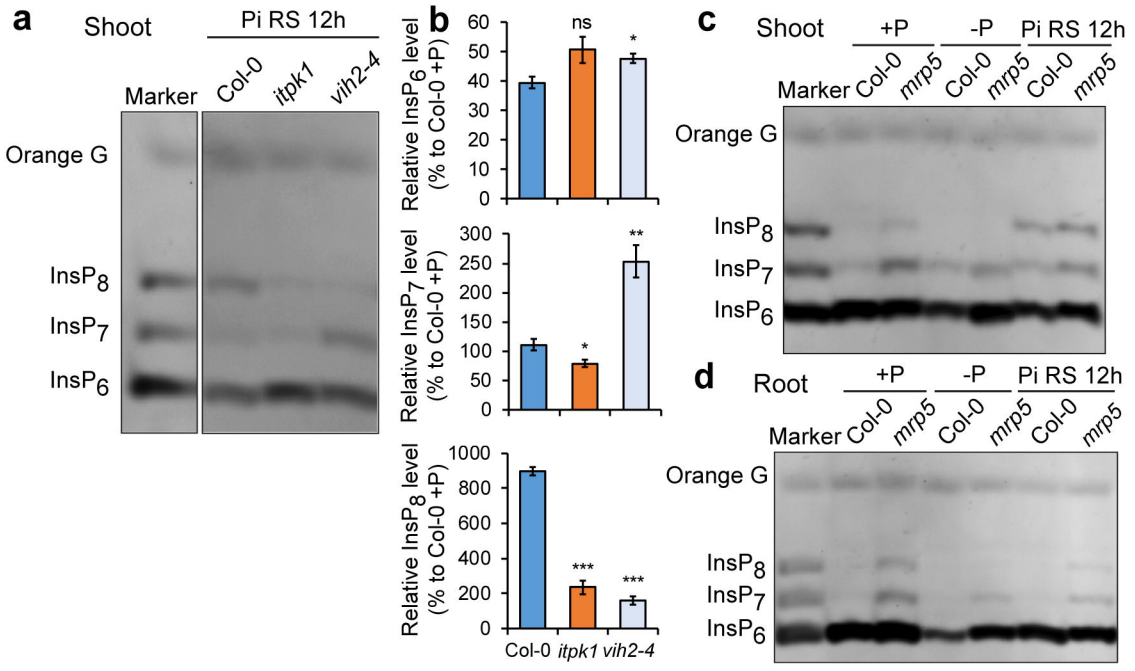

Fig. 3. ITPK1- and VIH2-dependent synthesis of PP-InsPs and dependency on $InsP_6$ compartmentation. **a-b** Loss of VIH2 increases $InsP_7$ levels in shoots. InsP detection in shoots of *Arabidopsis* WT, *itpk1* and *vih2-4* plants (**a**) and quantification of PAGE signals (**b**) 12 h after P_i resupply to P_i-starved plants in hydroponics. Data represent means ± SE ($n = 4$ biological replicates). $*P < 0.05$, $**P < 0.01$ and $***P < 0.001$ according to pairwise comparison with Student's *t*-test. **c-d** Impaired $InsP_6$ transport into the vacuole increases $InsP_7$ and $InsP_8$ levels in shoots and roots. InsP determination in shoots (**c**) and roots (**d**) of WT (Col-0) and *mrp5*. Plants were grown in hydroponics in P_i -sufficient solution (+P), exposed for 4 days to P_i starvation (-P) or resupplied with P_i for 12 hours (Pi RS 12h).

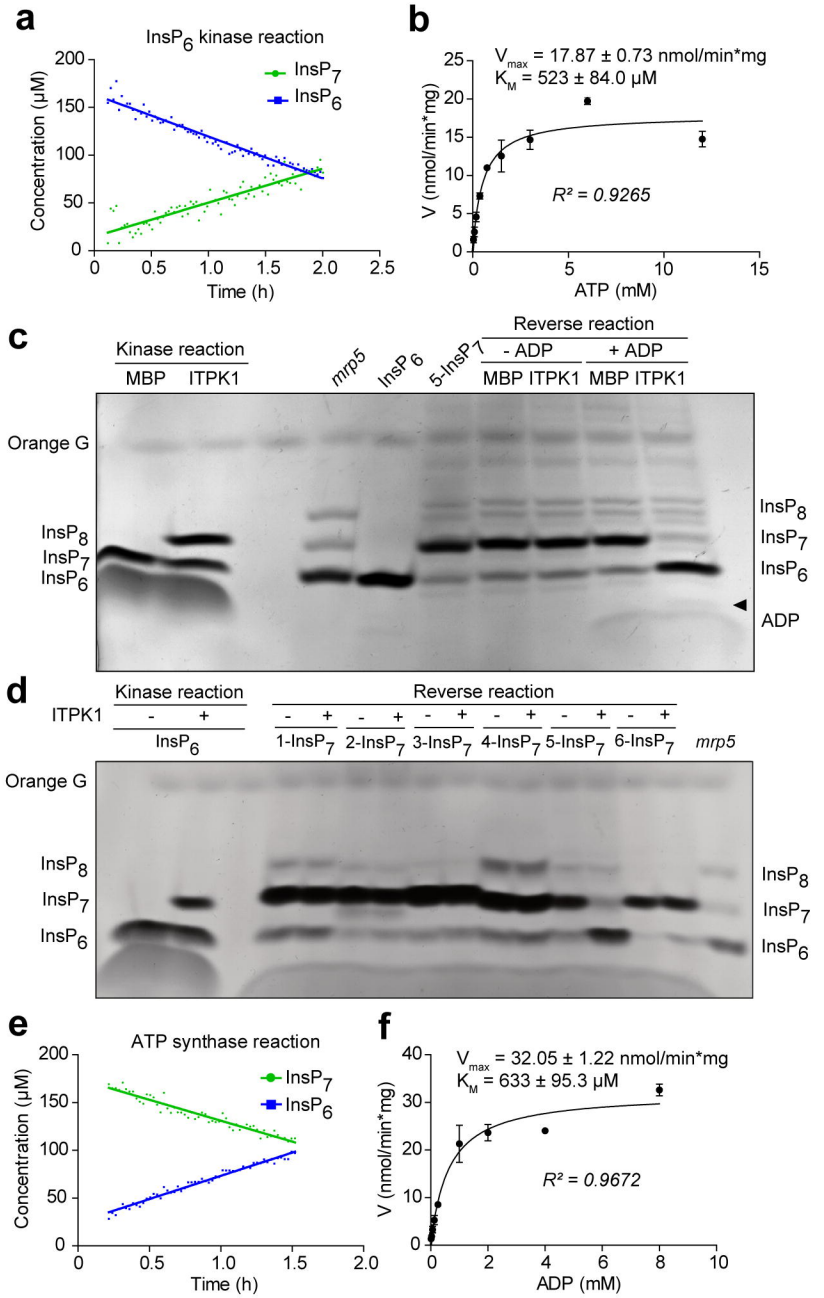

Fig. 4. *In vitro* characterization of ITPK1 activity.

a-b NMR analysis of InsP6 kinase activity of recombinant *Arabidopsis* ITPK1. Time-dependent conversion of $InsP_6$ to 5-$InsP_7$ (**a**) and reaction velocity determined at varying ATP concentrations (**b**). K_M and V_{max} were obtained after fitting of the data against the Michaelis-Menten model. **c-d** In the presence of ADP, recombinant *Arabidopsis* ITPK1 mediates 5-$InsP_7$ hydrolysis (**c**) but not the hydrolysis of other $InsP_7$ isomers (**d**). InsPs were separated via PAGE and visualized by Toluidine Blue staining. The identity of bands was determined by migration compared to $InsP_6$ and 5-$InsP_7$ standards and TiO_2-purified *mrp5* seed extract. $InsP_6$ kinase reaction served as positive control for the reverse reactions. Purified His_8-MBP tag (MBP) served as negative control for ITPK1. Arrowhead in **c**, indicates the presence of a small ATP band just above ADP. **e-f** NMR analysis of reverse reaction of recombinant *Arabidopsis* ITPK1. Accumulation of $InsP_6$ and conversion of 5-$InsP_7$ (**e**) and reaction velocity determined at varying ADP concentrations (**f**). K_M and V_{max} were obtained after fitting of the data against the Michaelis-Menten model.

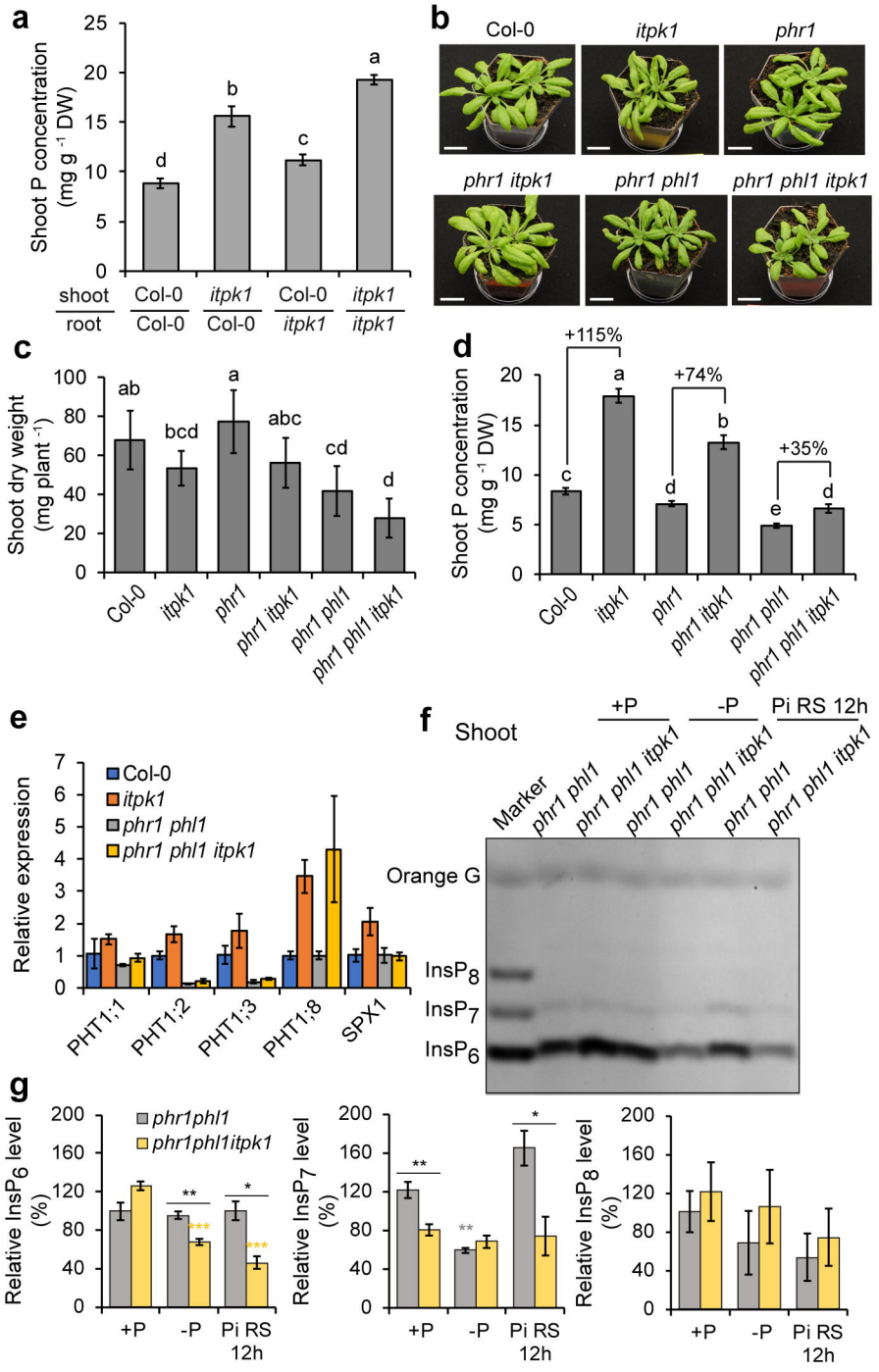

Fig. 5. P_i starvation responses are mainly regulated by ITPK1 activity in shoots.

a Total P_i concentration in shoots of self-grafted or reciprocally grafted WT (Col-0) and *itpk1*. Plants were grafted on agar plates and left recovering for 2 weeks. Positive grafts were transferred to peat-based substrate for another 2 weeks. Data represent means ± SD (n = 5-7 plants). **b-d** Genetic interplay between PHR1/PHL1 and ITPK1 in P_i sensing. Phenotype (**b**), shoot dry weight (**c**) and shoot P_i levels (**d**) of 3-week-old WT and indicated mutants grown on peat-based substrate. Data represent means ± SD (n = 6 plants). In **a**, **c** and **d**, letters indicate significant differences according to Tukey's test ($P < 0.05$). **e** ITPK1-dependent expression of P_i deficiency-induced genes in roots of the indicated P_i-sufficient plants. Data represent means ± SE (n = 4 replicates). **f-g** PHR1- and PHL1-dependent synthesis of InsPs as revealed by PAGE (**f**) and relative quantification of signals (**g**) in indicated double and triple mutants grown in hydroponics with P_i-sufficient solution (+P), exposed to 4 days of P_i starvation (-P) or resupplied with P_i for 12 hours (Pi RS 12h). Data represent means ± SE (n = 4 biological replicates). *$P < 0.05$, **$P < 0.01$ and ***$P < 0.001$ according to pairwise comparison with Student's t-test.

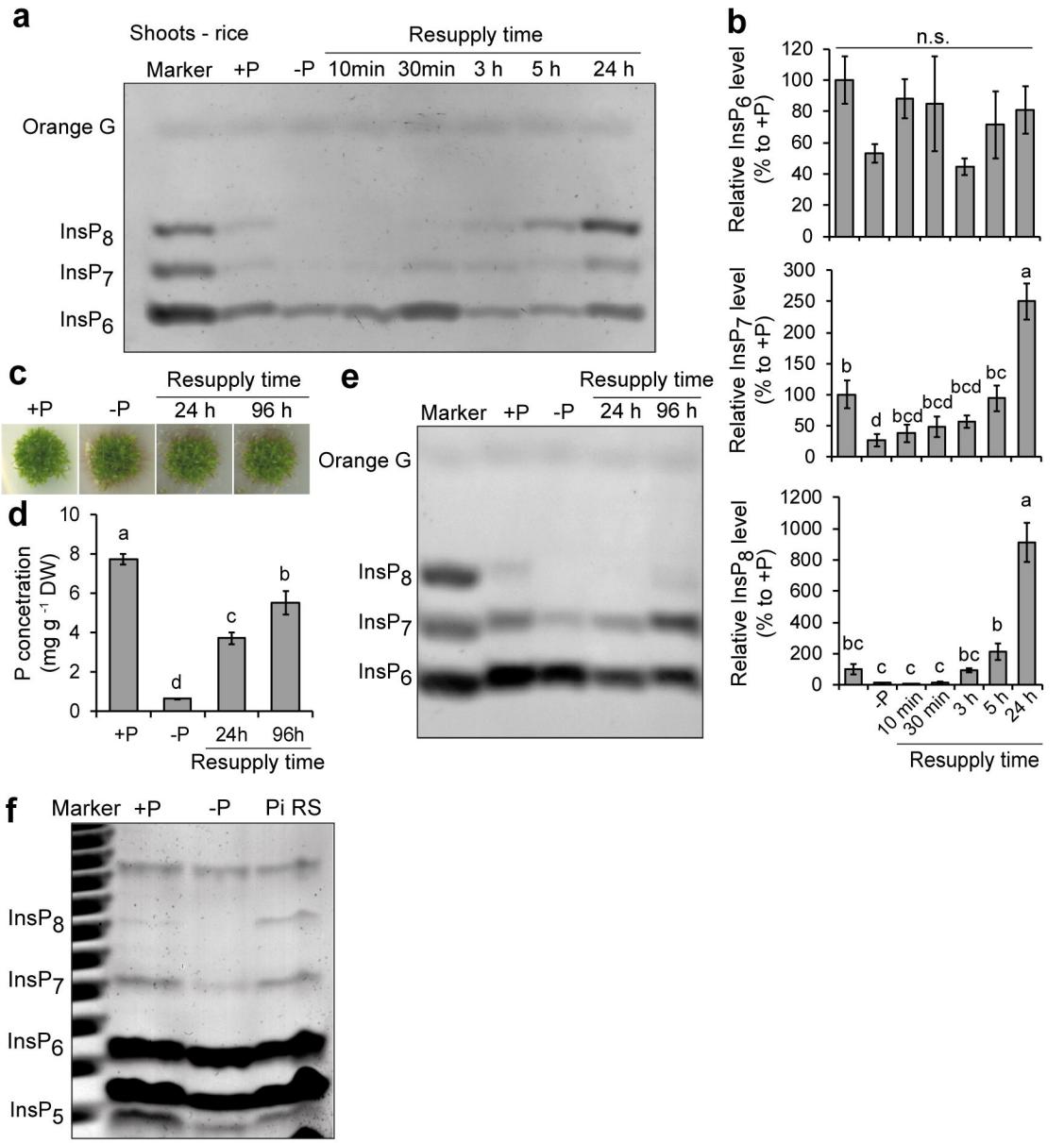

Fig. 6. P_i-dependent regulation of $InsP_8$ levels is conserved in multicellular organisms.
a-b Time-course analysis of InsPs in response to P_i starvation and P_i resupply in rice shoots. PAGE (**a**) and relative quantification of bands (**b**) of rice plants cv. Nipponbare grown in hydroponics. Data represent means ± SE ($n = 4$ biological replicates). Different letters indicate significant differences according to Tukey's test ($P < 0.05$). **c-e** Phenotype (**c**), total P_i levels (**d**) and PAGE of P_i-dependent synthesis of $InsP_7$ and $InsP_8$ (**e**) in gametophores of *Physcomitrella patens*. Plants were cultivated on sufficient P_i (+P), starved of P_i for 30 days (-P) or resupplied with P_i for the indicated time. Data represent means ± SD ($n = 3$ biological replicates). Different letters indicate significant differences according to Tukey's test ($P < 0.05$). **f** PAGE analysis of wild-type HCT116 cell extracts during P_i starvation and resupply. Cells were starved in P_i-free media for 18 h and resupplied with P_i for 3.5 h. Cells were harvested at the same time. The experiment was repeated twice with similar results.

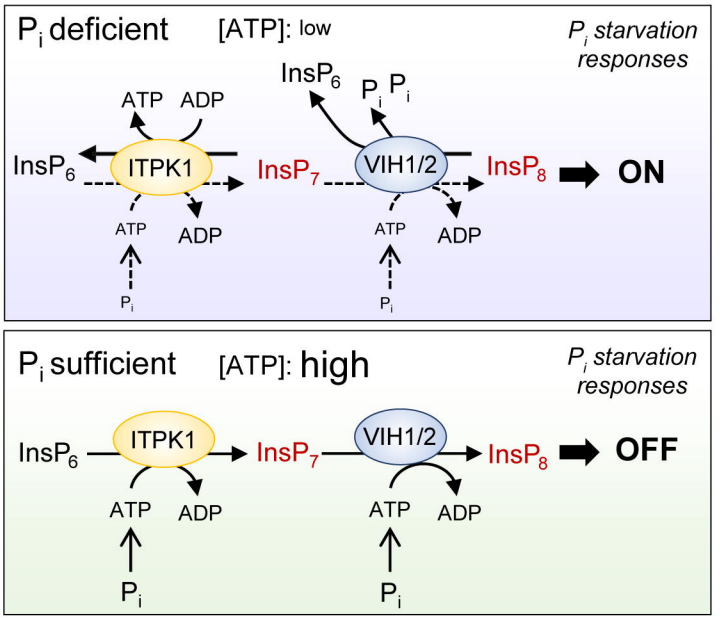

Fig. 7. Model for ITPK1-dependent generation and removal of InsP$_7$ and its link with VIHs and P$_i$ signaling. In P$_i$-deficient cells, low ATP levels stimulate ITPK1 to catalyze P$_i$ transfer from InsP$_7$ to ADP, thereby generating ATP and decreasing InsP$_7$. Decreased ATP and P$_i$ levels also activate the pyrophosphatase activity of VIHs to break down InsP$_8$. The removal of PP-InsPs destabilizes the association between PHRs and SPXs, allowing PHRs to induce P$_i$ starvation responses. When cells regain sufficient P$_i$, which increase ATP levels, ITPK1-mediated InsP$_6$ kinase activity is stimulated and the reverse reaction towards InsP$_7$ is inhibited. InsP$_7$ generated by ITPK1 serves then as substrate for InsP$_8$ production via the kinase domain of VIHs. As a consequence of increased PP-InsPs, SPX proteins recruit PHRs to repress P$_i$ starvation responses.